NTNU – Trondheim
Norwegian University of
Science and Technology

The Effect of Gas Kinetics on the Gas-Lift Efficiency for Viscous Oil in Vertical Pipe Flow

Carina Hoddø Steinbakk

Master of Energy and Environmental Engineering
Submission date: June 2015
Supervisor: Zhilin Yang, EPT

Norwegian University of Science and Technology
Department of Energy and Process Engineering

NTNU
Norwegian University
of Science and Technology

Department of Energy
and Process Engineering

EPT-M-2015-35

MASTER THESIS

for

Student: Carina Hoddø Steinbakk

Spring 2015

Effect of gas kinetics on the gas-lift efficiency for viscous oil vertical pipe flow
Effekten av gasskinetikk på gassløfteeffektivitet for viskøs olje vertikalt rør strømnings

Background and objective

The gas lift technology has been widely used in the oil and gas industry in both well and riser, in particular for light crude system. The purpose is to stabilise the flow, and to increase the production rate. The presence of more gas in vertical channel gives less gravitational pressure gradient, however, an increase in total volume flowrate gives more frictional pressure gradient. There is an optimum condition that the total flowrate of production fluid can be achieved.

For viscous oil field, the gas kinetics is one of the important physical phenomena that may influence significantly the gas-lift efficiency. Gas may be dissolved into oil or be released from the oil, this results in the variation of GOR in the oil, which also influence significantly the oil viscosity. Normally, it is assumed that the oil and gas are always in equilibrium state, if one gets the correct PVT information of the fluid, the gas-lift efficiency can be quantified reasonably. It has been found that the actual state is far from equilibrium, the time for reaching equilibrium state will depend on the type of fluid. The impact of non/equilibrium state of oil and gas on the gas-lift efficiency will be the focus of this work.

In this work, the physical models on the gas-lift for a vertical flowline will be developed, the coupling between the flow model and the non-equilibrium condition of fluid will be established.

The following tasks are to be considered:

1 Literature review of the gas-lift of viscous oil flow in a vertical pipe, the theory of gas lift for a vertical pipe flow should be reviewed
2 The gas kinetics of multi-component fluid should be documented, the theory of oil viscosity with relation to GOR and P.T. should be described
3 The coupling between flow model in a vertical pipe (a simple flow model for vertical gas-liquid flow) and PVT should be theoretically described
4 The model will be implemented in MatLab or other programming language, and relevant simulation should be conducted.
5. The analysis of the simulated results should be conducted in terms of non-dimensional physical parameters, from which the gas-lift efficiency can be estimated.

Within 14 days of receiving the written text on the master thesis, the candidate shall submit a research plan for his project to the department.

When the thesis is evaluated, emphasis is put on processing of the results, and that they are presented in tabular and/or graphic form in a clear manner, and that they are analyzed carefully.

The thesis should be formulated as a research report with summary both in English and Norwegian, conclusion, literature references, table of contents etc. During the preparation of the text, the candidate should make an effort to produce a well-structured and easily readable report. In order to ease the evaluation of the thesis, it is important that the cross-references are correct. In the making of the report, strong emphasis should be placed on both a thorough discussion of the results and an orderly presentation.

The candidate is requested to initiate and keep close contact with his/her academic supervisor(s) throughout the working period. The candidate must follow the rules and regulations of NTNU as well as passive directions given by the Department of Energy and Process Engineering.

Risk assessment of the candidate's work shall be carried out according to the department's procedures. The risk assessment must be documented and included as part of the final report. Events related to the candidate's work adversely affecting the health, safety or security, must be documented and included as part of the final report. If the documentation on risk assessment represents a large number of pages, the full version is to be submitted electronically to the supervisor and an excerpt is included in the report.

Pursuant to "Regulations concerning the supplementary provisions to the technology study program/Master of Science" at NTNU §20, the Department reserves the permission to utilize all the results and data for teaching and research purposes as well as in future publications.

The final report is to be submitted digitally in DAIM. An executive summary of the thesis including title, student's name, supervisor's name, year, department name, and NTNU's logo and name, shall be submitted to the department as a separate pdf file. Based on an agreement with the supervisor, the final report and other material and documents may be given to the supervisor in digital format.

☐ Work to be done in lab (Water power lab, Fluids engineering lab, Thermal engineering lab)
☐ Field work

Department of Energy and Process Engineering, 14. January 2014

Olav Bolland
Department Head

Zhilin Yang
Academic Supervisor

Research Advisor:

ABSTRACT

For heavy oil, artificial lift can be applied to increase and stabilise production flow. How the gas kinetics, i.e. the lift-gas composition will influence this increase is the subject of this thesis and will be described in relation to multiphase flow, pressure drop and pressure-temperature-volume (PVT) -theory.

A vertical pipe flow was studied, simulating the pressure drop coupled with the accompanying multiphase flow and PVT-information. The simulations were run in MATLAB, supported by NeqSim, a non-equilibrium simulation tool. NeqSim was used to acquire the local fluid parameters in order to calculate the local pressure drop. To study the gas lift efficiency, four different simulation variations were performed. Different lift-gas compositions were applied to the reservoir to observe the response. The bubblepoint pressure was altered by adjusting the composition, the bottomhole flowing pressure (BHFP) was lowered by adjusting the reservoir pressure, and a pressure delay was applied to simulate solution above the bubblepoint pressure and a dissolution process below the bubblepoint pressure. Two different pressure delays were implemented; one with equal delay, another with different delays.

These simulations were run on a well system with a heavy oil composition and a set geometry. The boundary conditions were the inlet and outlet pressures, set by the reservoir pressure, 120 bar, and the separator pressure, 15 bar. This locks the BHFP at 105 bar, but it was also adjusted for one of the simulation variations. The varying parameter was the gas injection rate, which is set by a for-loop in the code and input flow rate found by using the bisection method for each simulation.

From running the simulations and analysing the results it has been found that gas lift has a generally positive effect on the deliverability and stability of an oil field, though with an exceeding amount of gas lift injection the friction pressure drop will have a negative effect on production. A denser gas seems to give an increased gas lift efficiency due to the higher solubility rate. This makes optimising the injection rate imperative in order to have the highest possible production efficiency. There is a higher efficiency for an undersaturated reservoir, though requiring an increased gas injection rate. As for the composition of the lift-gas, it will have an impact on efficiency and should be taken into account. An increased solution effect implemented by a pressure delay will have positive effect on the lift efficiency. A denser gas will dissolve at

a higher rate into the liquid, decreasing the density of the wellbore column for higher gas injection rates than for the lighter gas. The delays occurring in a mass transfer situation between the phases will also influence the production, more so if the solution rate is higher than the dissolution rate, this should be studied further.

SAMMENDRAG

Kunstig trykkstøtte kan brukes for å øke og stabilisere produksjon for tungolje. Hvordan gassløft-komposisjonen til løftegassen påvirker denne økningen er hittil ikke veldig godt kjent og vil være tema for denne masteroppgaven. Dette vil også bli beskrevet i relasjon til flerfase-strømning, trykktap og trykk-temperatur-volum (PVT)-teori.

En vertikal rørstrømning ble studert, der trykktapet koblet med den tilhørende flerfasestrømningen og PVT-informasjon ble simulert. Disse simuleringene ble kjørt i MATLAB, støttet av NeqSim, et ikke-likevekts simuleringsverktøy brukt for å anskaffe de lokale fluid parameterne for å kalkulere det lokale trykktapet. Fire ulike simuleringsvariasjoner ble kjørt for å studere gassløft-effektiviteten. To forskjellige løftegass-komposisjoner ble tilført reservoaret og virkningen ble observert, boblepunkttrykket ble endret ved å tilpasse reservoarkomposisjonen, reservoartrykket ble senket, og til slutt ble en trykkforsinkelse påført for å simulere løselighet og fordamping over og under boblepunkttrykket. To ulike forsinkelser ble utøvd; en med lik forsinkelse og en med ulik forsinkelse.

Disse simuleringene ble kjørt på et brønnsystem med en tungolje-komposisjon og en gitt geometri. Grensebetingelsene var trykket inn og ut av systemet, satt av henholdsvis reservoartrykket, 120 bar, og separatortrykket, 15 bar. Dette fastsetter bunnhullstrykket på 105 bar. Som også varieres i en av simuleringsvariasjonene. Den varierende parameteren var gassinjeksjonsraten bestemt av en for-løkke i koden og masseraten til reservoaret som ble funnet gjennom halveringsmetoden (bisection method) for hver enkelt simulering.

Fra analysering av resultatene fra de kjørte simuleringene ble det funnet at gassløft har en generelt positiv effekt på et oljefelt, spesielt for et undermettet reservoar, men trenger da enda høyere gassinjeksjons rater. Når det gjelder komposisjonen til løftegassen vil den ha en innvirkning på løfte-effektiviteten, hvor lettere gasser gir en økning i produksjonen sammenlignet med de tyngre gassene, og bør derfor tas hensyn til. En tyngre gass vil kondensere raskere inn i væskefasen, noe som vil senke tettheten til væskesøylen mer enn for den lettere injeksjonsgassen. En økt kondenseringseffekt implementert gjennom en trykkforsinkelse vil ha en positiv effekt på løft-effektiviteten Forsinkelsene som oppstår i situasjoner med masseoverføring mellom fasene vil også påvirke produksjonen, spesielt der hvor ekspansjonsraten er høyere enn for kondenseringsraten. Dette bør studeres videre.

PREFACE

ACKNOWLEDGEMENTS

There are many aspects of writing a thesis, some more important than others. A few of them being knowledge, motivation, creativity, a strong work ethic and inspiration. Most important is the help and support one gets from an academic supervisor. I wish to thank my supervisor, Zhilin Yang, for his patience, support and for motivating me to push my own academic and personal boundaries. He has been a key ingredient in helping me becoming an independent researcher. I also would like to thank Even Solbraa at Statoil ASA, my NeqSim-guide, always ready to help and contribute to a solution for the problem at hand. For some key input in the fields of gas lift and multiphase flow, I would like to thank Jianbo Yang at Mariner, Statoil UK and Arne Valle at Statoil ASA.

A special note of appreciation goes out to Frank-Are Steinbakk, OMT (Operations and Maintenance Technology) Manager, Mariner, Statoil UK; my dad, mentor and source of guidance, inspiration and comfort. Further, I must thank my good friends and colleagues Tina Louise Langeland and Hanne Jorunn Trydal, for letting me pester them with questions and concerns. I addition, I would like to thank Charlotte Hundewadt for her input.

Last, but not least, I would like to thank the rest of my family for their constant encouragement and support.

THESIS TECHNICALITIES

This thesis is submitted in fulfilment of the requirements for the degree of Master of Science at the Department of Energy and Process Engineering (EPT), Norwegian University of Science and Technology (NTNU). The work has been carried out for the Industrial Process Technology programme under the Energy and Environment degree at NTNU. The master's education programme involves two years of foundation courses and two years of courses in varying areas of energy and processing. The last year of the five-year degree has contained a research project supported by research courses for one academic semester before culminating in the semester for the master thesis.

CONTENTS

LIST OF FIGURES

LIST OF TABLES

NOMENCLATURE

LIST OF ACRONYMS

BHFP	Bottom Hole Flowing Pressure
EPT	Energy and Process Engineering
ESP	Electrical Submersible Pump
GOR	Gas Oil Ratio
MATLAB	Technical Computing Software
NeqSim	Non-Equilibrium Simulator
NTNU	Norwegian University of Science and Technology
PVT	Pressure-Volume-Temperature

LIST OF SYMBOLS

Symbol	*Name*	*Formula*
μ_g	Gas viscosity [kg/ms]	
μ_l	Liquid viscosity [kg/ms]	
μ_m	Mixed viscosity [kg/ms]	$\mu_l v_l + \mu_g v_g$
ρ_g	Gas density [kg/m^3]	
ρ_l	Liquid density [kg/m^3]	
ρ_m	Mixed density [kg/m^3]	$\rho_l v_l + \rho_g v_g$
ΔP	Length of pipe section [m]	$\frac{Pipe\ length}{No.of\ grids}$
A	Pipe cross-sectional area [m]	$\frac{\pi D^2}{4}$
C_0	Distribution coefficient	
C1	Methane	
C2	Ethane	
C3	Propane	
C6-C30	Heavy hydrocarbons	
cp	Centipoise (viscosity unit)	
f	Friction factor	$f_{lam} = \frac{64}{Re}$ $f_{turb} = 0.316 Re^{-\frac{1}{4}}$

g	Local acceleration due to gravity [m/s^2]	9.81
iC4	Isobutane	
P	Pressure [bar]	
P_{wf}	Bottom Hole Flowing Pressure	
Q	Mass flow rate [kg/s]	
Q_g	Gas mass flow rate [kg/s]	$w_g Q$
Q_l	Liquid mass flow [kg/s]	$w_l Q$
Q_{vg}	Gas volume flow rate [m^3/s]	$\frac{Q_g}{\rho_g}$
Q_{vl}	Liquid volume flow rate [m^3/s]	$\frac{Q_l}{\rho_l}$
Q_{vm}	Mixed volume flow rate [m^3/s]	$Q_{vg} + Q_{vl}$
Re	Reynolds Number	$Re = \frac{(\rho V_{mix}\, D)}{\mu}$
T	Temperature [K]	
U_0	Drift velocity [m/s]	
U_m	Mixed superficial velocity	$U_{sl} + U_{sg}$
U_{sg}	Superficial gas velocity [m/s]	$\frac{Q_g}{A\rho_g}$
U_{sl}	Superficial liquid velocity [m/s]	$\frac{Q_l}{A\rho_l}$
v_g	Gas volume fraction	Non-slip: $\frac{Q_{vg}}{Q_{vm}}$ Slip: α
v_l	Liquid volume fraction	Non-slip: $\frac{Q_{vl}}{Q_{vm}}$ Slip: 1 - α
w	Mass fraction	
w_g	Gas mass fraction	
w_l	Liquid mass fraction	
x	Mole fraction	
x_g	Gas mole fraction	
x_l	Liquid mole fraction	

Z	Compression factor	
α	Void fraction	$\frac{V_g}{V_l + V_g}$
σ	Surface tension [N/m]	
H	Liquid holdup	

1 INTRODUCTION

1.1 MOTIVATION AND RELEVANCE

The background for this thesis is the need for gas lift in nearly depleted wells. As the reservoir continues to be depleted, the pressure goes down and more gas expands, which causes the density and viscosity of the reservoir fluid to increase. The static pressure drop then increases and production slows down. Gas lift is a method used to increase the bottomhole flowing pressure (BHFP) in the well, decreasing the static pressure drop by decreasing the density and thereby increasing the production in an oil well.

Today exist many oilfields that are depleting, and the low BHFP makes it uneconomical to maintain production due to the low yield. Gas lift can resume production as long as there is source gas available, increasing yield and revenue. With oils that are more viscous there is the issue of how the oil responds to gas injection and a need to discover how lift-gas interacts with such a fluid. In addition, finding the optimal gas injection rate will be prudent to keep production at the highest level of efficiency.

When developing oil fields in deep sections under the seabed, there can occur complications coupled with the static pressure drop. This problem can be solved by using artificial lift, like electric submersible pumps (ESPs) or gas lift. Gas lift will be governed by non-equilibrium thermodynamics relations between the liquid- and gas phase. How fast this gas is dissolved into the oil will decide the holdup in the well and risers, and thereby the static pressure drop, which sets the limitations for the gas lift efficiency. There is a very limited knowledge of the effect gas lift has on the production efficiency when used on viscous oil today.

Gas lift technology has been used widely in the oil and gas industry in both well and riser, but mostly for light crudes. It is used to stabilise the flow and to increase the liquid flow rate. With gas injected into the vertical channel the static pressure gradient will decrease, but the frictional pressure gradient will increase with increasing gas injection rates. This technology can beneficially be transferred to oilfields that are more viscous.

As mentioned, the gas lift response will be dominated by the non-equilibrium thermodynamics between oil and gas, caused by the dissolution delay. The rate of dissolution will be dependent on flow parameters and gas injection rate. The gas molecules' ability to dissolve at the given pressure and temperature is also important, which will be regulated by the rate of diffusion, where the composition of the gas and oil will come into play.

The disturbance of the equilibrium that occurs when gas lift is applied is illustrated in Figure 1. A pressurised container is filled with a two-phase mixture of oil and gas. By applying a high rate of additional gas, the equilibrium is displaced, starting a transfer of gas into the oil phase. As time passes, the system will settle into a new equilibrium, where some of the gas has dissolved in the oil.

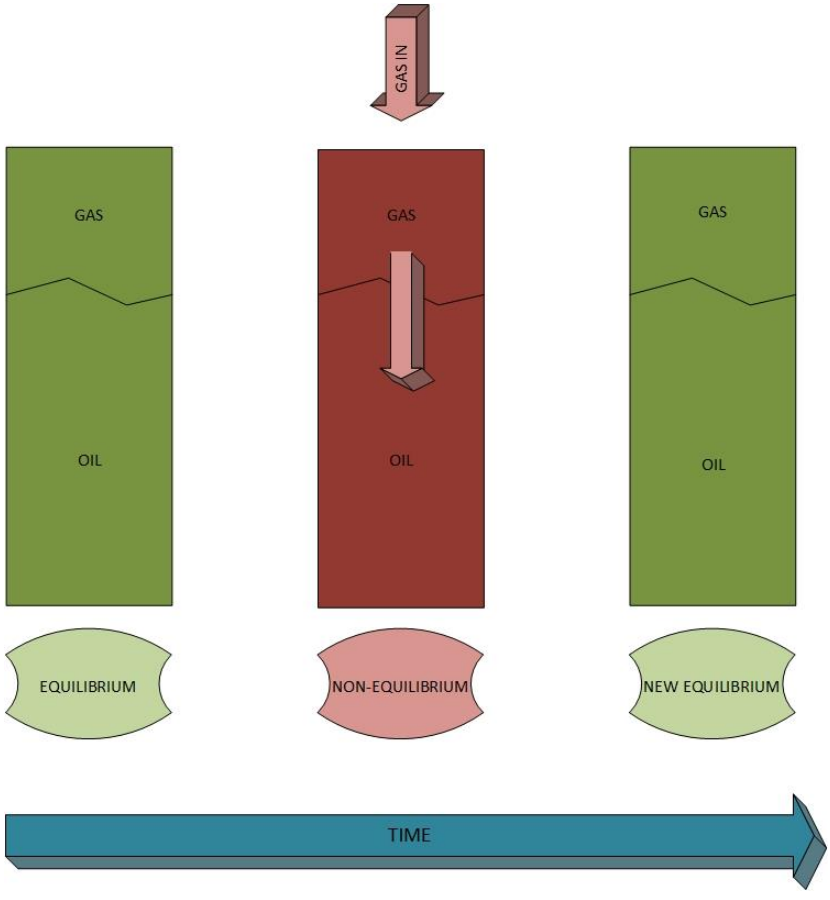

Figure 1 Thermodynamic Equilibrium Description

As new oilfield developments will be at deeper and more challenging depths, the static pressure gradient will increase. This will create more need for artificial lift, and there is a great potential for gas lift in such fields. By being able to better understand and predict the well behaviour of the mass transfer between gas and oil, the oil production can be greatly enhanced (Solbraa, E., 2015).

Using artificial lift when producing a heavy crude has become essential for keeping up the efficiency and keeping oil reservoirs economically sustainable. Gas lift as an artificial lift method, is amongst the preferable options as long as there is source gas available, however, gas compositions might influence the gas lift efficiency. This has been researched to a certain degree, though not to the extent of how the composition of the lift-gas and the different components might interact with the reservoir production fluid. This thesis will study the possible positive and negative effects the lift-gas composition can have on the lift efficiency.

1.2 OBJECTIVES

1. Literature review of the gas lift of viscous oil flow in a vertical pipe and the theory of gas lift for a vertical pipe flow is reviewed.

2. The gas kinetics of multi-component fluid is documented and the theory of oil viscosity in relation to gas oil ratio (GOR) and PVT is described.

3. The coupling between flow model in a vertical pipe (a simple flow model for vertical gas-liquid flow) and PVT is theoretically described.

4. The model is implemented in MATLAB, which is then coupled with NeqSim.

1.3 SCOPE

In this thesis, the hydrodynamic model for two-phase gas-liquid flow is implemented into a MATLAB-code, which is also coupled with Non-Equilibrium Simulation tool, abbreviated to NeqSim. In the model, a two-phase flow model explore the thermodynamic and hydrodynamic flow variations due to different compositions, altered bubblepoint and reservoir pressure, and an inlaid pressure delay. The model includes the numerical Bisection-method.

1.4 THESIS LAY-OUT

The thesis is structured as follows:

- In Chapter 2 an introduction of gas lift and its necessity due to a less productive pressure gradient precedes a general overview of multiphase flow, with the pressure drop, flow type and flow regimes described. It also covers the PVT-relations, connecting the GOR, gas kinetics and viscosity in regards to the gas lift efficiency.
- Chapter 3 introduces the mathematical model for pressure drop in a vertical pipeline, followed by the selection of the optimal void fraction correlation for a non-ideal flow scenario.
- Chapter 4 present the simulation tool NeqSim used in this thesis, with the description of the modules and routines it utilises.
- Chapter 5 proceeds to introduce the computer code written in MATLAB used to run the simulations. The code has been compartmentalised in order to describe each of main processes' functionalities and the chapter is rounded off with an overall process flowchart combining each of the parts to form the whole the simulation code.
- Chapter 6 elaborate upon the different simulation variations, with an overview of how the results will be presented and which important models will be used during the simulations.
- Chapter 7 ensues with the results for the hydrodynamic simulation results and a discussion. Then follows the thermodynamic simulation results with a corresponding discussion. Each discussion-section ties together the discoveries made in the result-sections and discusses them in relation to the theory established earlier in the thesis, commenting on the variations.
- Chapter 8 closes with conclusions and expounds on the limitations of the work done and possible future work. This comprises of expanding the model to include a more complex geometry and further advancing the code to include a transport model, with heat transfer and temperature variations.

2 GAS LIFT FUNDAMENTALS FOR VISCOUS OIL WELLS

Vertical pipe flow is a complex system with several factors and conditions affecting the deliverability. This chapter will discuss the important areas when handling such a flow, focusing on the addition of gas lift to the wellstream. Section 2.1 discusses multiphase flow, a vital part of understanding the behaviour of a pipe flow. The interaction between the liquid and gas flow will be an imperative part of discovering how gas lift will influence the pipe flow, and especially how the pressure drop in the pipe will develop. Furthermore, Section 2.2 discusses gas lift in detail, before Section 2.3 introduces the gas kinetics of the pipeline, and will cover how the GOR and oil viscosity relates to each other. The complexity of understanding and predicting pipe flow relies on each of these areas. All of them are independent of each other, but interrelated through influencing the flow and gas lift efficiency. The fluid discussed in this thesis will be a two-phase flow, consisting of gas and oil, modelled as a single-phase flow.

2.1 MULTIPHASE FLOW

In this section, the specifics of multiphase flow will be introduced; detailing the pressure drop and the different flow regimes for vertical flow.

2.1.1 Flow Regimes

There are generally four different flow regimes for vertical pipe flow, shown in Figure 2 (Takács, 2005). This thesis will focus on bubble flow, modelling the two-phase flow after single-phase flow assumptions. The simulation results can be affected by disturbances in the flow, f. ex. transitioning from bubble flow to slug flow due to an increase in gas velocity, creating more turbulence in the flow.

- *Bubble flow*: Low to medium gas flow velocities, the gas phase is made up of uniformly distributed bubbles rising in the continuous liquid phase. The gas bubbles have a higher velocity than the liquid, which will result in slip between the phases.
- *Slug flow*: The liquid phase present in bubble flow and dispersed bubble flow starts to diminish, and it becomes a succession of large (Taylor) bubbles and liquid slugs.

- *Churn flow*: With an increase in gas velocity, the Taylor bubbles will increase in size, and the gas content of the liquid slugs will increase. This will cause the gas void fraction to reach a critical point and the liquid slugs will collapse, lifted by small, distorted Taylor bubbles.
- *Annular flow*: Occurs at high gas velocities. The gas phase is continuous in the pipe core, while the liquid travels up the pipe wall as a film and some bubbles remain entrained in the core of the pipe.

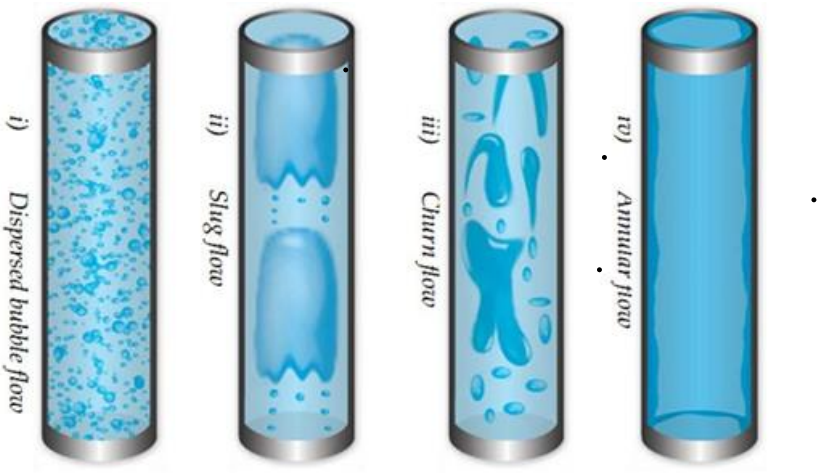

Figure 2 Flow Regimes (Bratland, 2010)

2.1.2 **Pressure Drop**

When working with oil wells, there will be multiphase flow in the wellbore, which induce challenges that are a big side effect of oil production. If the gas lift technology is to be applied in highly viscous oil wells, there are parameters that have to be taken into account, which will affect the efficiency of the well production, shown in Figure 3 (Takács, 2005).

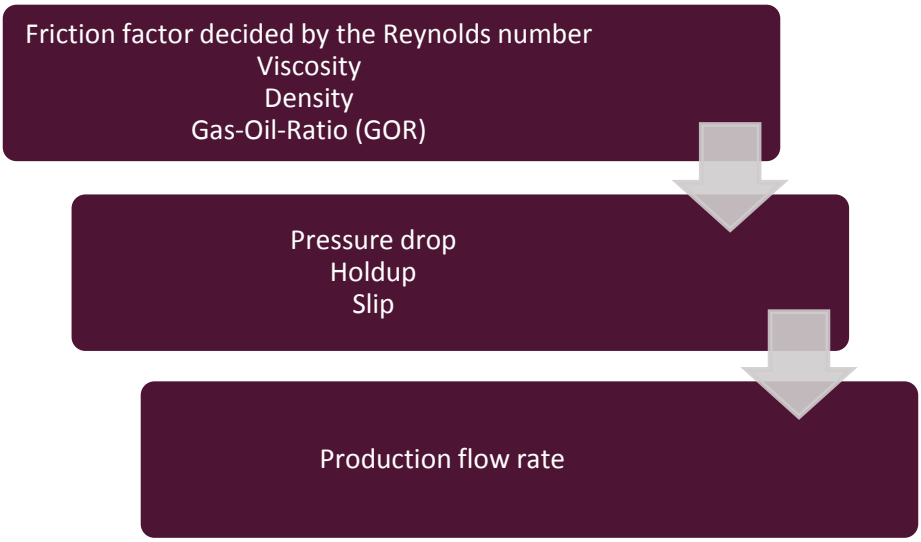

Figure 3 Factors for Production

The governing relation for the efficiency of gas lift is the pressure drop since it is directly related to the power requirements of the compressor, pump or bottomhole pressure to maintain flow. When dealing with the pressure drop, three separate elements are taken into account, shown in Equation 1:

$$\frac{dP}{dh} = gravitational\ gradient + frictional\ gradient + acceleration\ gradient \quad (1)$$

The gravitational or static gradient supports the gas and liquid gradient in the vertical pipe. As for the frictional gradient, it represents the drag of the flowing mixture on the pipe-wall only. The last term, acceleration gradient, is often very small, so it can be neglected for flow in wells (Ros, 1961).

A pressure drop due to viscous effects, or the frictional gradient, represents an irreversible pressure loss, which is proportional to the viscosity of the fluid. This pressure loss can be expressed for laminar, turbulent, smooth or rough surfaces, horizontal and inclined pipes as shown in Equation 2, where f is the Darcy friction factor.

$$\Delta P_f = \frac{f L \rho V_{avg}^2}{2D}, \quad (2)$$

In the analysis of piping systems, pressure loss is commonly expressed in the terms of equivalent fluid column height, called the head loss, or the static or gravitational gradient. The head loss is caused by viscosity, and is shown in Equation 3, where ρ denotes the fluid density in kg/m^3, g is the acceleration of gravity and h the height of the fluid column.

$$\Delta P_g = \rho g h \tag{3}$$

Gravity has no effect on flow in horizontal pipes, but it has a significant effect on both the velocity and the flow rate in inclined pipes. The additional force will be the component of the fluid weight and the pressure drop is changed to

$$\Delta P_g = \rho g L \sin\theta, \tag{4}$$

where L is the length of the pipe. In the case of this study, the pipe will be vertical with an inclination of 90°, which reduces the pressure drop to

$$\Delta P_g = \rho g L. \tag{5}$$

In inclined pipes, the combined effects of pressure difference and gravity drives the flow, where gravity helps downhill flows, but opposes uphill flows. Therefore, much greater pressure differences need to be applied to maintain a specified flow rate in uphill flow, although this becomes important only for liquids, because the density of gases is generally low (Çengel & Cimbala, 2006).

To obtain the frictional pressure drop, a friction factor is used. For a smooth pipe inner surface, there will be much less impact on the flow than for a pipe with a rough surface, meaning the friction factor will be simplified, not accounting for any roughness in the pipe. Such correlations will be used for both the laminar and turbulent flow. For laminar flow, Darcy's friction factor will be applied, shown in Equation 12. This is not to be confused with the Fanning friction factor, which is four times smaller than the Darcy friction factor. While for turbulent flow, the Blasius friction factor correlation is used, shown in Equation 13. The Blasius correlation is appropriate for the simulations in question, as it is eligible for flows with Reynolds numbers up to 10^5.

When using the friction factor for both laminar and turbulent flows, the friction factor will decrease for a hydraulic smooth pipe, shown in the Moody diagram in Figure 4.

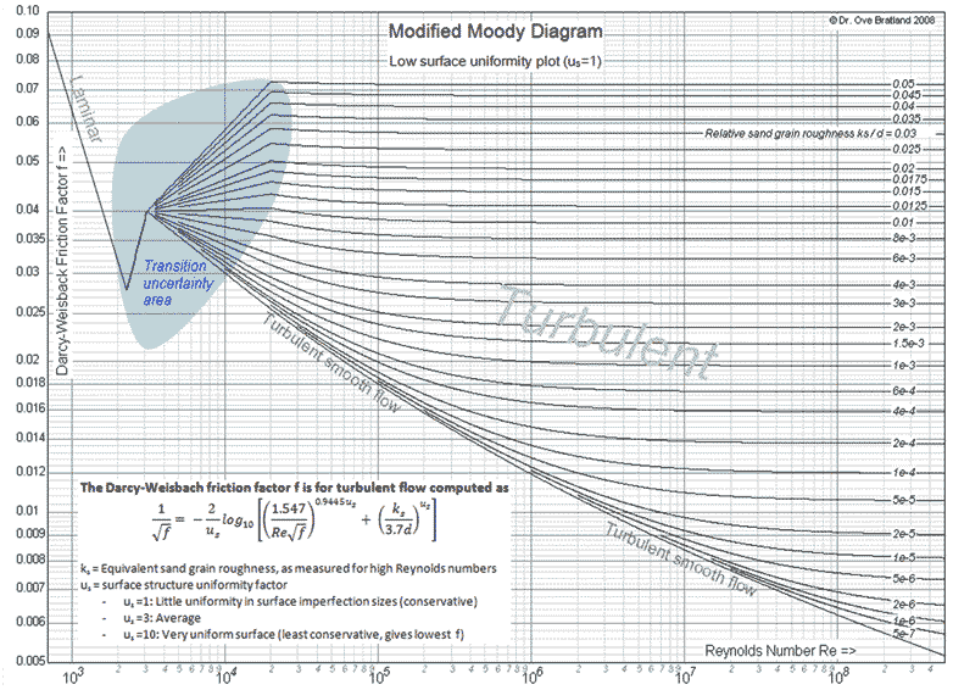

Figure 4 Moody Diagram (Bratland, O., 2009)

It can be seen that for Re < 2100 the flow will be laminar, before it enters a transitional area. Here the friction factor will be assumed the same as for turbulent flow, though, the behaviour of the flow in this area is very uncertain. For Re > 4000 the flow will be fully developed turbulent flow and the friction factor will here also decrease for increasing flow rates. The friction factor displayed in the Moody Diagram is the implicit Darcy-Weisbach friction factor for turbulent flow, but as mentioned, the Blasius friction factor will in this thesis be used instead, which is eligible for smooth pipes.

2.1.3 Multiphase Flow Models

There is a large variation, as mentioned, of flow regimes in pipelines, also when it comes to time and length scales. Therefore there exists a range of computational models for calculating the pressure drop and other important parameters. These are empirical relations, based on empirical data as well as phenomenological or mechanistic models. These relations are based on physics, for example forces, turbulence, mass and momentum transfer. Here it is also possible to take the flow regimes into account. It also has to be considered if the model will be transient or steady state, where a transient model will give the time evolution of the variables along the pipe.

Since the system is two-phase flow, there is two possible approaches to modelling the fluid. There is the two fluid model, which uses momentum equation for each field, and is therefore suitable for separated flows. This model needs the contribution of wall and interface friction relations. The simplified approach is the mixture, or drift flux model. This model uses a mixture momentum equation, and is appropriate to use for mixed or assumed homogeneous flow, such as a bubbly flow. The model needs to have a mixture wall friction relation and a slip relation. For this thesis the mixture model will be used, and is further discussed in Section 3.1. The slip relation is detailed in Section 3.1.2. While the friction model was introduced in Section 2.1.2.

2.2 GAS LIFT

In this section, general gas lift theory will be detailed, along with the importance of the pressure gradient in relation to gas lift efficiency.

2.2.1 Background

A typical oil field will have three main stages: primary, secondary and tertiary production. The first will include depleting the natural reservoir pressure, producing up to 20% of the field's capacity. After this, the reservoir pressure needs to be maintained to extract more oil. At the tertiary stage, the reservoir pressure is usually too low and the well is dead, meaning the reservoir pressure is no longer sufficient to overcome the hydrostatic pressure created by increased viscosity of the reservoir fluid. It is at this stage that artificial lift will be of use, which can lead to a 30 to 60 percent increase of the total capacity. (Shabbir, 2014).

It is becoming increasingly necessary to use artificial lifting of oil. Especially for wells with heavy oil artificial lift will be crucial for maintaining production. It has also become more apparent that popular artificial lift techniques like gas lift and electric submersible pump may be less effective when handling heavy oils, due to the rise in viscosity. When it comes to using gas lift, it is very flexible within the gas injection rate ranges it is capable of producing, and with the source gas available. The downsides is that this source gas has to be available at all times and it can be less effective with viscous oils (Brown, 1981).

2.2.2 Gas Lift Process

The process of gas lift, illustrated in Figure 5, is straightforward; lift-gas is injected into the well stream at a low position in the wellbore, which results in a decrease in overall density of the wellbore column. This will decrease the gravitational pressure drop, but also increase the frictional pressure drop, making it a fine balanced art finding the right injection rate for maximum production. With the injected gas, the BHFP is reduced and will therefore give a preferential pressure difference (Takács, 2005), creating an upswing in production. The BHFP is the located at the bottom of the wellbore, making up the difference between the separator pressure and reservoir pressure. This pressure drop is thus created by the frictional and static pressure drop, and will need help to overcome said pressure drop if the BHFP is too low. The lift-gas can be applied either intermittently or continuously, depending on the wellstream.

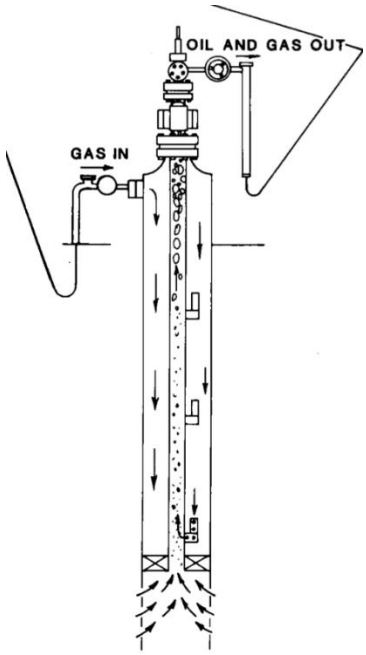

Figure 5 Schematic of Gas Lift well (Hu, 2005).

2.2.3 Pressure Gradient

An important parameter when applying gas lift is the pressure gradient of the well. The accurate data for the pressure gradient during flow of oil and gas in a vertical pipe can be used to determine optimum flow in the pipe and the pressure drop very much determines the production rate. The fact that the pressure drop decreases when the gas flow through the pipe increases is well known, the reason being that with increasing velocities the total flow gets more turbulent mixing the gas flow with the liquid and also makes the gas flow more slowly though the liquid and thereby decreasing the static head. When increasing the gas injection rates, the wall friction will increase, adding to the frictional pressure drop. The minimal pressure drop can be obtained from using a certain pipe cross-section, where an increasing pipe diameter will decrease the flow rate, meaning there is an optimal pipe diameter for the most efficient flowrate. For the purpose of this thesis, the pipe diameter will be kept constant at 0.177 m. In the case of gas lift, a certain injection rate of gas can maximise production. There has been much research done on this subject, though less on low pressure and low production wells, and with viscous oils (Turner, Hubbard, & Dukler, 1969).

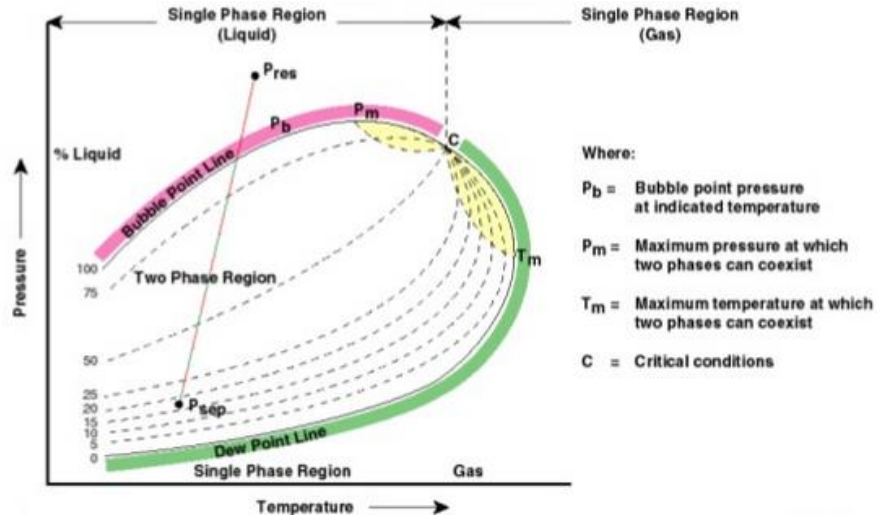

Figure 6 Two-Phase Envelope (Shell, 1999)

As the pressure in the pipe decreases, the reservoir fluid will flow up the wellbore, and when it reaches the bubblepoint pressure, it will separate into two phases, shown as the two-phase region in Figure 6. This pressure loss is caused by the pressure gradients in the wellbore, namely the frictional and static pressure drop.

Low-potential wells have low velocities producing low wall friction values, slip loss due to low liquid speed, and high gas speed due to high buoyancy, which all give contributions to the pressure loss. In addition, the liquid viscosity will have an impact on the pressure drop, both for gravitational and frictional losses (Ros, 1961). According to a study done by Hagedorn & Brown in 1964, it was shown that the liquid viscosity had little effect on the pressure gradients for two-phase vertical flow when the liquid viscosity was lower than 12 cp (0.012 kg/ms). For a value exceeding this, an impact on the production would be made.

2.3 PVT-Relations

This section will introduce the behaviour of the two-phase flow in regards to change in composition and the relation of the pressure to the bubblepoint. It is then tied together with the fluid's gas-oil-ratio and viscosity.

2.3.1 Gas Kinetics and GOR

There has been little research into the kinetics of lift-gas and well composition, and how it might influence gas lift efficiency. It was however shown by A. Maijoni and A. Hamouda in 2011 that heavier lift-gas gives larger production rates compared to lower gas density for dynamic simulations, while the opposite is true for steady state simulations. Which components make up the ideal gas composition will be an interesting research study, and will be lightly approached in this thesis, mainly focusing on methane and isobutane.

When dealing with an oil reservoir, the behaviour of the oil becomes very important. The oil can be undersaturated, meaning it is at a reservoir pressure above the bubblepoint pressure, saturated, which is at the bubblepoint pressure, leaving the under saturated level below the bubblepoint pressure. The PVT-specification of the mixture can therefore help to predict the well's performance and how the oil will interact with the gas injected into the wellbore.

The composition of the oil in the reservoir is the source of the PVT-information, like the bubblepoint pressure and viscosity. The path of the pressure for a general reservoir is shown in Figure 7. The figure shows how the pressure travels from the undersaturated area via the bubblepoint pressure line and into the under-saturated area.

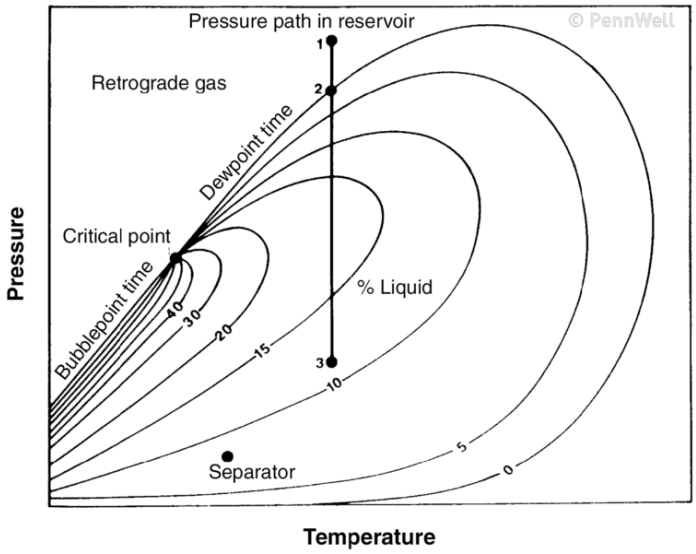

Figure 7 Pressure Development in Reservoir (Rivera, 2008)

This path can be further explained by the four phases an oil reservoir goes through as it is being produced (Conaway, 1999). All due to the reservoirs pressure in relation to the bubblepoint, or saturation pressure, in a gas driven reservoir shown in Figure 8.

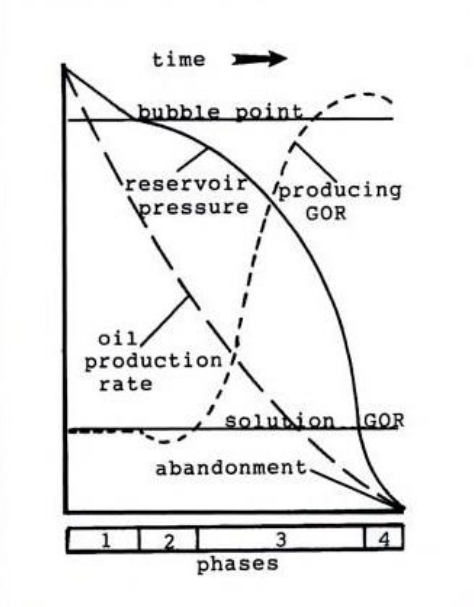

Figure 8 Stages of GOR (Conaway, 1999)

Phase 1: As production starts, the reservoir will be undersaturated and consist of oil alone. The pressure will decline rapidly towards the bubblepoint pressure. All of the gas is dissolved in the oil, thereby making the producing GOR the same as the solution GOR.

Phase 2: Due to the gas coming out solution, the producing GOR will dip under the solution GOR as the pressure reaches the bubblepoint pressure. This gas is not produced, as the critical gas saturation is not yet reached. The pressure decline will be slowed because of the expansion of gas, giving a portion of free gas in the pipe.

Phase 3: Free gas is produced along with the oil and the remaining solution gas as the critical gas saturation is exceeded. As the decreasing pressure liberates more solution gas, the producing GOR increases. The expansion of oil, but mostly the expansion gas is the principal drive mechanism, governed by the pressure drop. The slower pressure decline will slow the decrease in the oil production rate, but the relative permeability effects of the increasing gas saturation and decreasing oil saturation will in turn accelerate this. As phase three progresses, the pressure will drop more rapidly due to a higher gas production rate.

Phase 4: Here the production reaches its economic limit, as the remaining oil is dead - confirmed by the downward turned production GOR. This type of reservoir is a good candidate for secondary recovery such as gas lift technology.

Thus, the effect of the gas expanding as the pressure declines is the increase of GOR. As the reservoir pressure reaches the bubble point pressure, it will decline quickly due to high compressibility of the gas expanding. When the bubbles begin to flow, the producing GOR can increase to as much as ten times the initial GOR. As the reservoir pressure continues to fall, the GOR will eventually start to decline as the gas expands less and less. When the GOR rises the oil production rates will fall, and wells will need artificial lift to sustain them (AAPG, 2014).

2.3.2 Oil Viscosity

To predict the production of the reservoir, the composition can reveal essential PVT-information. From this, certain necessary characteristics of the oil can be determined, for use in a prediction model. One of these characteristics is the oil viscosity (Çengel & Cimbala, 2006).

Oil viscosity is a parameter used in reservoirs and flow lines which is needed to calculate movement of fluids. It is closely related to the producing GOR, as with more gas expanding and coming out of solution, the more the viscosity will

increase, and with an increase in dissolved gas there will be a decrease in viscosity.

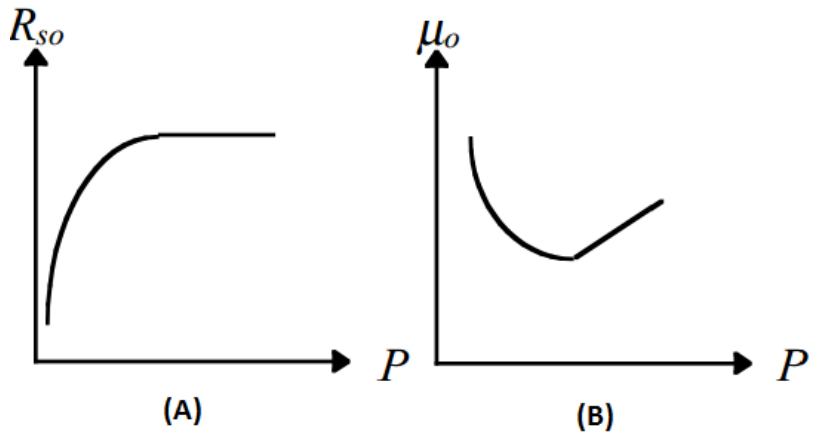

Figure 9 GOR and Viscosity through Production Stages (Kleppe, 2015)

The solution gas-oil ratio will increase with increasing pressure until it reaches the bubblepoint pressure and for undersaturated oil conditions it will remain constant (A). The oil viscosity will decrease for increasing pressure before it reaches bubblepoint pressure, where after it will increase nearly linearly with increasing pressure (B), shown in Figure 9. Normally, the lift-gas efficiency will be reduced with increased viscosity, as the gravitational pressure drop increases and the productivity reduces (PetroWiki, 2014).

3 MODEL DEVELOPMENT & NUMERICAL SIMULATIONS

The simulations will be run for a vertical pipe flow, modelled in Section 3.1. The model is based on the pressure drop model presented in Section 3.1.1, and will be coupled together with the Non-Equilibrium Simulation software, NeqSim, introduced in Chapter 4. The software will present the local fluid parameters found through a PVT-flash at each local grid of the pipe, to the MATLAB-code. This couples the PVT-information with the multiphase model, enabling a way to follow and analyse the flow behaviour based on pressure changes in the pipeline.

3.1 MODELLING

The mathematical model for the pipe simulation, along with the four different void fraction correlations and the drift flux model accounting for the slip between the two phases will be explained in this section. The bisection method used to numerically decide the correct flow rate for the simulations is described in Appendix D.

Since this is two-phase flow, which is a more complicated flow system, certain assumptions are made. This is because the following models were developed for single-phase pipe flow only and it requires the following corresponding assumptions. Homogeneous flow is assumed, keeping the application of the single-phase frictional pressure gradient applicable and the use of mixture properties is necessary. No heat or mass transfer is accounted for, leaving a simplified model for testing the effect of gas lift on the deliverability of the system only.

To calculate the mixture density for the Reynolds number in the simulation code, the mixture velocity calculated from the superficial velocities is used, shown in Equation 9. These are the velocities the given phase would have if it were flowing alone in the pipe. This is demonstrated in Figure 10. Where U_{LS} is the superficial liquid velocity and U_{GS} is the superficial gas velocity. Together they make up the mixture velocity, calculated by Equation 6, 7 and 8. Where Q_L an Q_G is the mass flow rate for liquid and gas, respectively and q_L and q_G is the volume flow rate for the liquid and gas phase, respectively. The mixture velocity is used alongside

the mixture values for viscosity and density in order to calculate the Reynolds number.

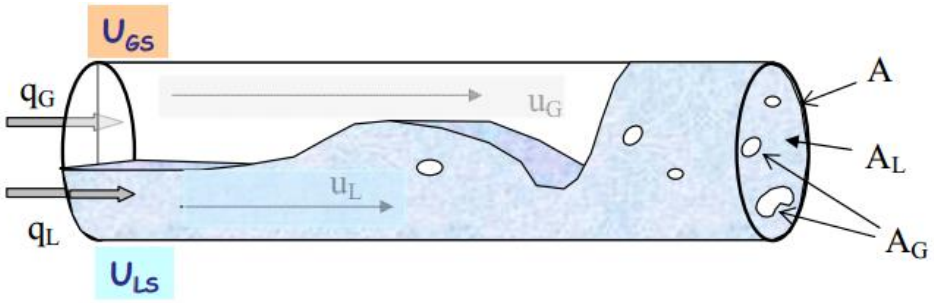

Figure 10 Visualisation of Superficial velocity (Aker Solutions, 2011, May 31st)

$$U_{LS} = \frac{q_L}{A} = \frac{Q_L}{A\rho_L} \tag{6}$$

$$U_{GS} = \frac{q_G}{A} = \frac{Q_G}{A\rho_g} \tag{7}$$

$$U_{mix} = U_{LS} + U_{GS} \tag{8}$$

For the mixture density and mixture viscosity, Equation 10 and 11 is used, respectively. Where α describes the void fraction, or gas fraction, and H is the liquid fraction, or oil fraction, in the pipe.

$$\rho_m = \alpha\rho_g + H\rho_l \tag{9}$$

$$\mu_m = \alpha\mu_g + H\mu_l \tag{10}$$

3.1.1 Pressure Drop Model

In this study, there will be performed simulations in a vertical wellbore. The production flow rate will be calculated by using the following mathematical model for vertical pipe flow assuming homogeneous flow, constant temperature, no heat or mass transfer and steady state conditions, combined with the bisection method, explained in Appendix D (Sawhney, G.S., 2011)

.

The model accounts for the Reynolds number:

- Laminar flow: Re < 2100
- Turbulent flow: Re > 2100 (including the transitional area between laminar and turbulent flow).

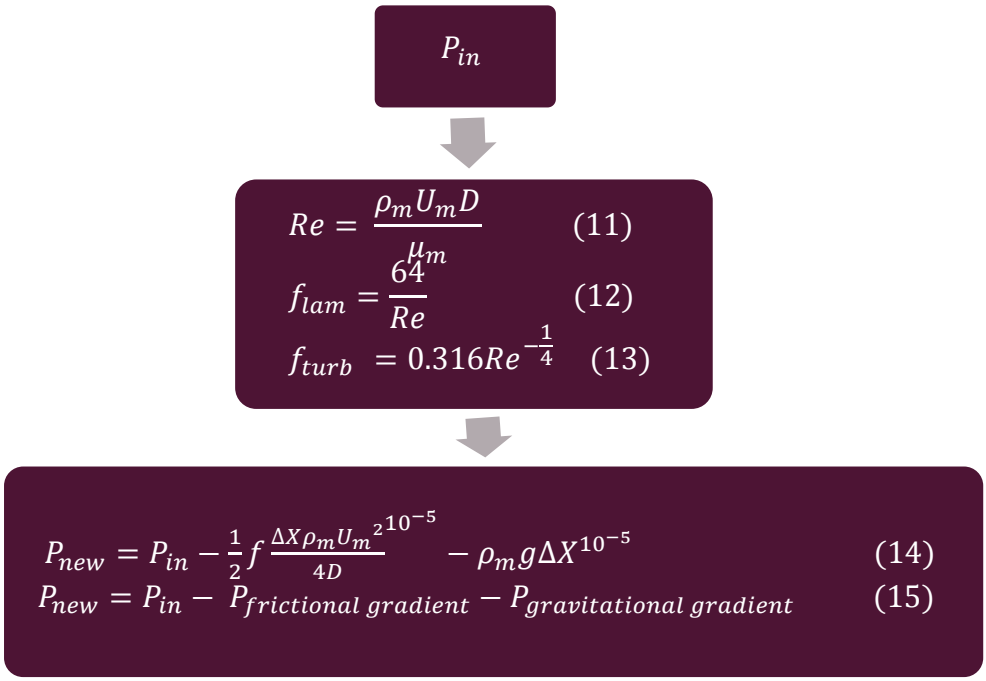

Figure 11 Mathematical Model for Vertical Pipe Flow

As Figure 11 shows the models input is the pressure, and the model calculates the frictional and gravitational pressure drop for the respective part of the pipe, based on the theory presented in Section 2.1.2. It then subtracts this pressure drop from the input pressure, giving the new pressure.

3.1.2 Drift Flux Model and Void Fraction Correlations

Calculating the pressure drop in a non-ideal situation requires accounting for the slip, so alongside the ideal situation with a no-slip relation, referred to as Equilibrium in this section's figures, four different void fraction correlations were used when running simulations, combined with the most popular drift flux model. These are shown in Table 1.

Table 1 Void Fraction Correlations and Drift Flux Model

Void Fraction Correlations		
Zuber-Findlay	$C_0 = 1.2$	(16)
	$U_0 = 1.53\left(\frac{g\sigma\Delta\rho}{p_l^2}\right)^{\frac{1}{4}}$	(17)
Jowitt	$C_0 = 1 + 0.796exp\left(-0.061\sqrt{\frac{\rho_l}{\rho_g}}\right)$	(18)
	$U_0 = 0.034\left(\sqrt{\frac{\rho_l}{\rho_g}} - 1\right)$	(19)
Bestion	$C_0 = 1$	(20)
	$U_0 = 0.188\sqrt{\frac{gD\Delta\rho}{\rho_g}}$	(21)
Zhilin Yang	$C_0 = 1$	(22)
	$U_0 = 1.53\left(\frac{g\sigma\Delta\rho}{p_l^2}\right)^{\frac{1}{4}}$	(23)
Drift flux model		
	$\alpha = \frac{U_{sg}}{C_0(U_{sg} + U_{sl})U_0}$	(24)

Each correlation includes a distribution coefficient, C_0 and a drift velocity, U_0 which are incorporated into the code. The drift flux model also denotes U_{sg} and U_{sl}, superficial gas and liquid velocities respectively (Zhilin Yang et al, 2005).

When choosing which void fraction correlation to work with, the simulations were run without and with injection gas entering the production stream - focusing on the latter because this is the objective of this thesis. The optimal performance is of course of interest, that is, high production rate with as low local void fraction as possible for the most stable conditions. The ideal void fraction correlation would be able to handle all flow regimes accurately, accounting for slip in the vertical pipe setting. Of course, conditions are subject to change, so more than one correlation could be appropriate for the different simulations. For simplicity's sake, one correlation will be chosen to work with.

Figures 12, 13 and 14 show the flow rates for all correlations, the hold-up and the void fraction along the wellbore, respectively. The 'Equilibrium'-entry in Figure 12 accounts for the no-slip holdup scenario and is not an eligible contender as it is next to impossible to achieve no-slip conditions (liquid and gas travelling at the same velocity).

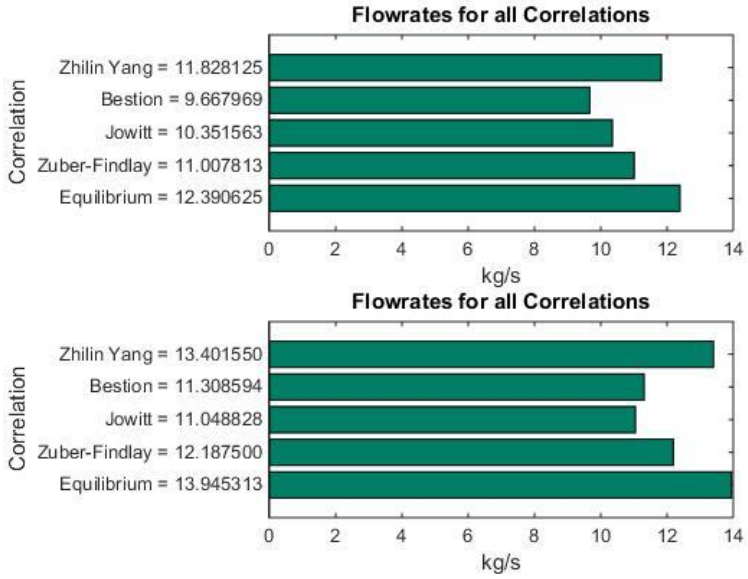

Figure 12 Flow rate Comparison for Void Fraction Correlations

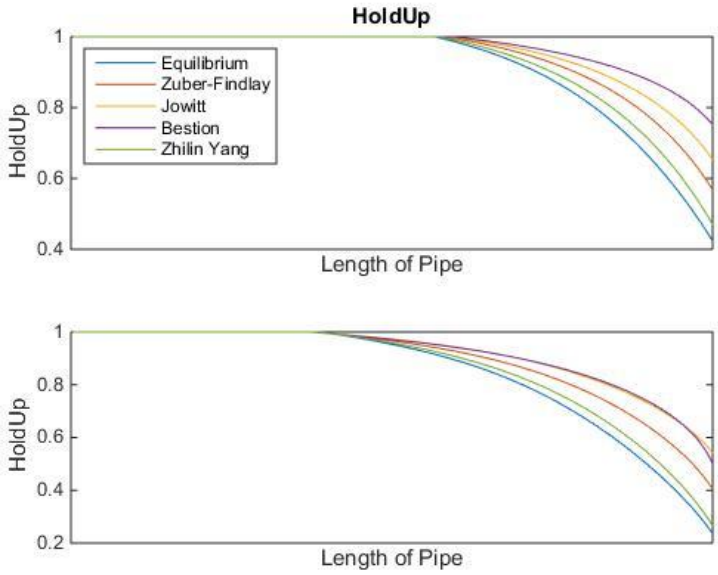

Figure 13 Hold-Up Comparison for Void Fraction Correlations

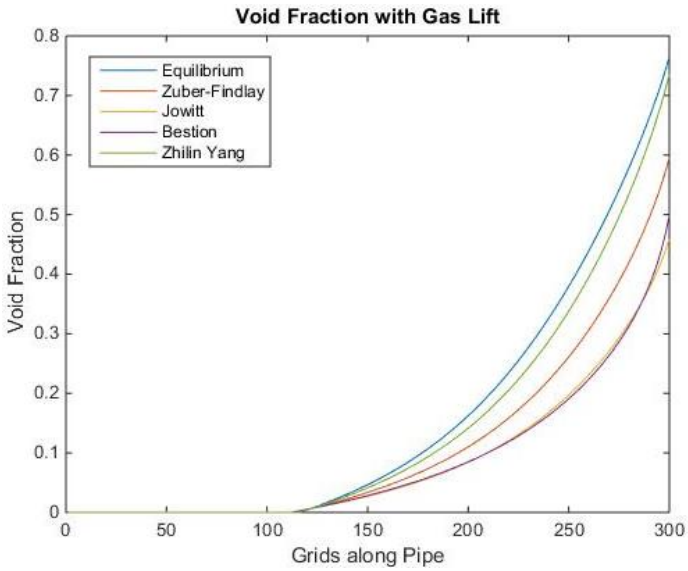

Figure 14 Void Fraction for Void Fraction Correlations

When injecting gas each correlation has its own specific bubblepoint pressure. This is because each correlation will give a different volume fraction, which in turn will give its own pressure decrease for each iteration. When this is reapplied to the composition normalisation with accompanying flow rate the overall composition will be slightly different, giving a different bubblepoint pressure.

Figure 15 shows how the bubblepoint differs with and without injected gas. The void fraction, as seen in Figure 14, for each correlation corresponds to the difference in bubblepoint, the lowest void fraction giving the highest saturation pressure.

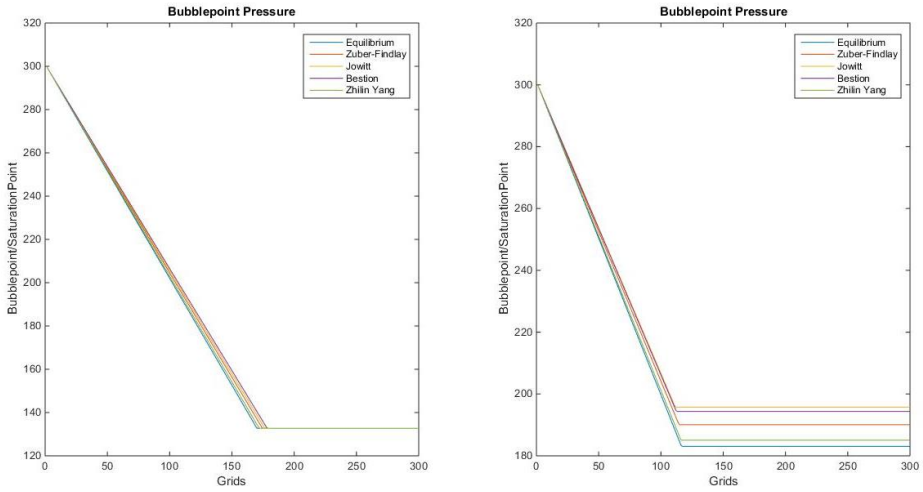

Figure 15 Bubblepoint Development With and Without Gas Lift

The Zhilin Yang-correlation gives the highest flow rate, showing a positive response with an 11.74% increase between no gas lift and with gas lift. It has the lowest holdup, meaning it has a high gas flow. In Figure 15, it can be seen that this correlation also gives the lowest bubblepoint pressure for the given composition, maintaining a higher pressure for a longer period.

While the Bestion- and Jowitt-correlations have high hold-up along the pipeline, they have a lower production rate. Though the Bestion-correlation responds well to gas lift, it has an unstable tendency with higher gas injection rates, giving numerical errors in the simulation.

The closest contender to the Zhilin Yang-correlation is therefore the Zuber-Findlay-correlation, which gives a relatively high production rate, though only a 9.68% increase when gas lift is applied. It has a higher hold-up along the pipe, and naturally, has the second lowest bubblepoint.

Even though the local holdup is low for the Zhilin Yang-correlation, the production is high and responds well to gas lift.

From this point on, the chosen correlation will be the Zhilin Yang-correlation.

4 NEQSIM

To simulate the complex behaviour of a well system, the proper parameters for the model are needed, such as local density, viscosity, mole fraction and so on. To get these, the Non-Equilibrium Simulator software known as NeqSim is utilised and coupled with the MATLAB-code. This provides the needed information for each iteration. NeqSim is developed by Even Solbraa at Statoil and the Department of Refrigeration and Air Conditioning at the Norwegian University of Science and Technology (NTNU).

4.1 WHAT IS NEQSIM?

NeqSim is a dynamic process simulator specially designed to handle non-equilibrium situations. These thermodynamic equilibrium-processes include common non-equilibrium processes such as absorption, distillation, and multiphase flow in pipelines, drying processes, hydrate formation and heat exchange. The software also handles traditional equilibrium process calculations (equilibrium separators, equilibrium streams).

NeqSim can be applied to:

- Equilibrium calculations (TPflash / PHflash / TVflash)
- Multiphase flash calculations
- Chemical equilibrium calculations (reactive equilibrium)
- Electrolyte calculations (salts, amines)
- Hydrate calculations (TP-flash, phase curves)
- One phase pipe flow / Two phase flow (steady state / transient)
- Absorption / Distillation (steady state / transient)
- Freezing point calculations
- Construction of Thermodynamic Property Charts (2D / 3D)
- Parameter fitting (thermodynamic / fluid mechanics data)

4.2 NEQSIM-MODULES

NeqSim is based upon six base routines or modules; the thermodynamic-, fluid mechanical-, physical properties-, chemical reaction-, parameter fitting- and GUI module. They will each be elaborated upon in the following subsections.

4.2.1 Thermodynamic Routines

4.2.1.1 Models

NeqSim's thermodynamic library contains the following models:

- SRK Equation of State
- Peng Robinson Equation of State
- Schwartzentruber Equation of State
- Furst & Renon Electrolyte Equation of State
- CPA Equation of State (SRK-CPA and PR-CPA)

4.2.1.2 Mixing rules

NeqSim uses the following mixing rules:

- Classic – no interaction parameters
- Classic with interaction parameters
- Huron-Vidal Mixing Rule (NRTL)
- Modified Huron Vidal Mixing Rules (NRTL)
- Wong Sandler mixing Rules
- Combinational rules for the CPA-EoS

New thermodynamic models can easily be added to the database.

4.2.2 Fluid Mechanical Routines

4.2.2.1 Equipment

The fluid mechanic equipment are divided into the subsequent sections:

- Segments (one or more legs)
- Legs (one or more nodes)
- Nodes

4.2.2.2 Fluid Mechanical Models

The fluid mechanic model is a one-dimensional one or two-phase transient flow model. NeqSim solves the conservation equations simultaneously by iteration. These equations are:

- Conservation of total mass (pressure and phase fractions)
- Conservation of momentum (velocities)
- Conservation of energy (temperatures)
- Conservation of components (components)

4.2.2.3 Unit Equipment

NeqSim can solve the following unit operations:

- Pipe flow (one / two phase)
- Reactor flow (distillation / absorption)

4.2.3 Physical Properties Routines

NeqSim calculates the following physical properties for fluids:

- Viscosity (dynamic / kinematic)
- Conductivity
- Diffusion Coefficients (Fick / Maxwell Stefan)
- Surface tension

4.2.3.1 Models

It is possible to choose among many models for all physical properties. Most of the models are taken from the book Molecular Properties of Liquids and Gasses (Prausnitz et.al.).

4.2.4 Chemical Reaction Routines

4.2.5 Parameter Fitting Routines (including experimental database)

NeqSim uses the non-linear Levenberg-Marquardt parameter-fitting model. Examples in the GUI show how to do parameter fitting to experimental data. A database with collected (and public) experimental data is distributed along with the program (NeqSim Access database).

NeqSim supports Monte-Carlo Simulations for predicting errors in fitted parameters.

4.2.6 GUI module

4.3 PROGRAMMING LANGUAGE

NeqSim is written in Java and is easily extendible with new modules. It also implements Python as a scripting language – a powerful, easy and object oriented language. Fast and easy Python scripts are automatically made with the toolbars in the GUI. NeqSim uses the Jext text-editor and the VisAd scientific visualisation library (NeqSim, undated).

5 THE NUMERICAL IMPLEMENTATION

This section will cover the overview and description of the programming code, which is described in Appendix C. The code has been divided into four main processes. Process 1 describes the composition variation, through flow rate and lift-gas input. In Process 2, the pressure delay option is outlined. Process 3 shows the mathematical model, while Process 4 covers the bisection method. Each process will be defined in the beginning of each subsection. A general outline is described at the end of the chapter.

As for the system itself, it is modelled as a frozen, steady state system. That is, the inlet and outlet pressures are set as boundary conditions, locking the BHFP. This will give only one correct flowrate, which the system will find. This will be altered after how much injection gas is added to the system.

5.1.1 Process 1: Flow rate and Composition

In this process, shown in Figure 16, all the outlining parameters are set, most importantly inlet and outlet pressure. In addition, the composition is defined, both for reservoir and lift-gas. With these compositions, a new mixture is defined, with the flow rates of the respective fluids the new composition is normalised and set as the main fluid. The unit for the flow rate input is kg/s. The tolerance for the results is set at 0.1 and the model operates with 300 grids. The gas injection rate will be set here, the unit in kg/s.

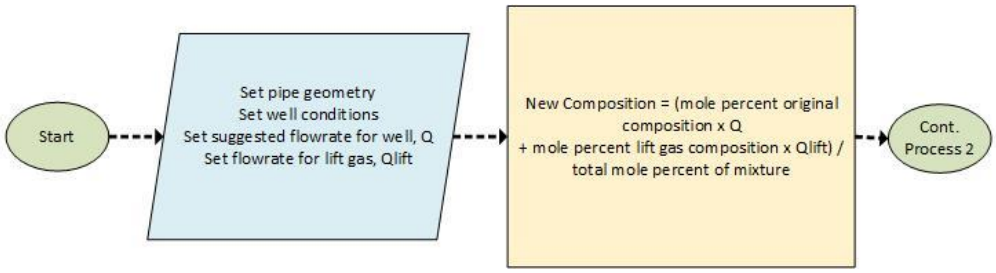

Figure 16 Process 1: Flow rate and Composition

5.1.2 Process 2: Pressure Delay

If a solution or dissolution process is to be simulated this happens in Process 2, illustrated in Figure 17. If the pressure taken into the process is over the bubblepoint pressure, a small pressure addition is added, mirroring a solution process. Reversely, if the pressure is below the bubblepoint pressure, the pressure is reduced by a small fraction, simulating a dissolution process. If the pressure is at the bubblepoint pressure, there will be no change.

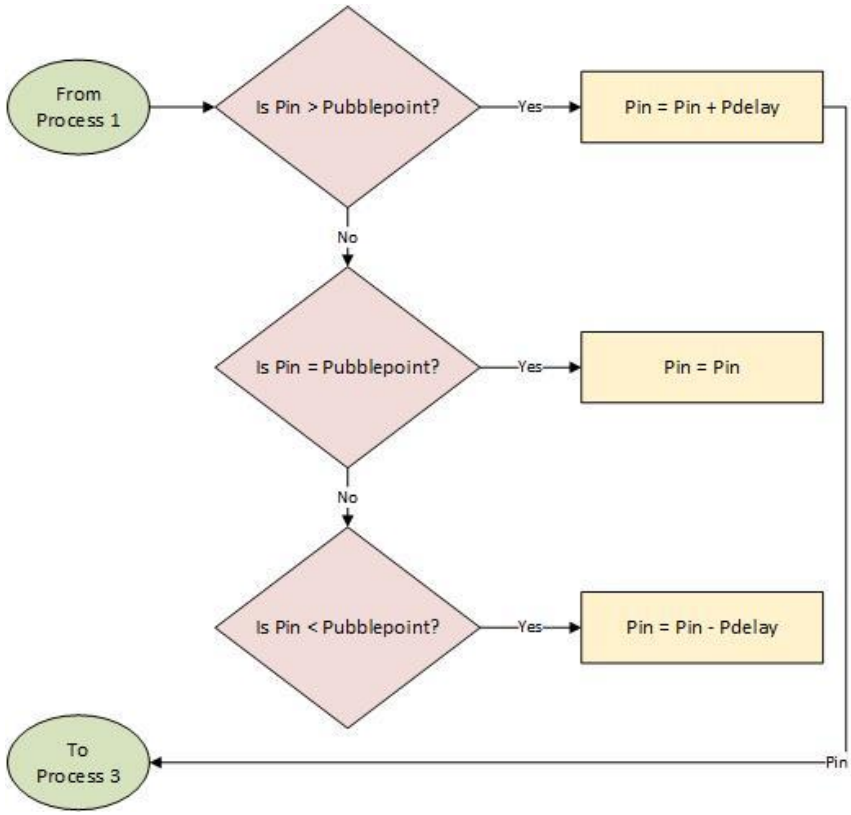

Figure 17 Process 2: Pressure Delay

5.1.3 Process 3: Mathematical Model for Pressure Drop

Figure 18 shows Process 3, where the main result is a pressure reduction. This reduction is for each grid-section of the wellbore. From inlet at the bottom of the well to the outlet, the pressure will be reduced at each grid, calculating the pressure drop from local fluid parameters acquired from NeqSim and the chosen void fraction. At the top of the well, after all the grids have been accounted for,

the code will check the sign of the new pressure. If this is negative, the flow rate is too high, and will be reduced before restarting at Process 1.

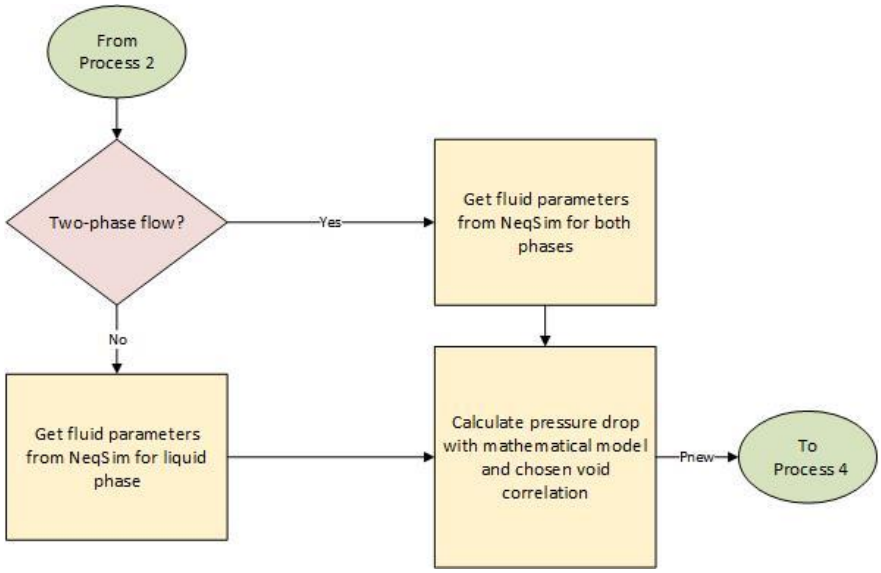

Figure 18 Process 3: Mathematical Model for Pressure Drop

5.1.4 **Process 4: Bisection Method**

Process 4 implements the bisection method, described in Appendix D, in order to find the correct flow rate for the given composition. See Figure 19.

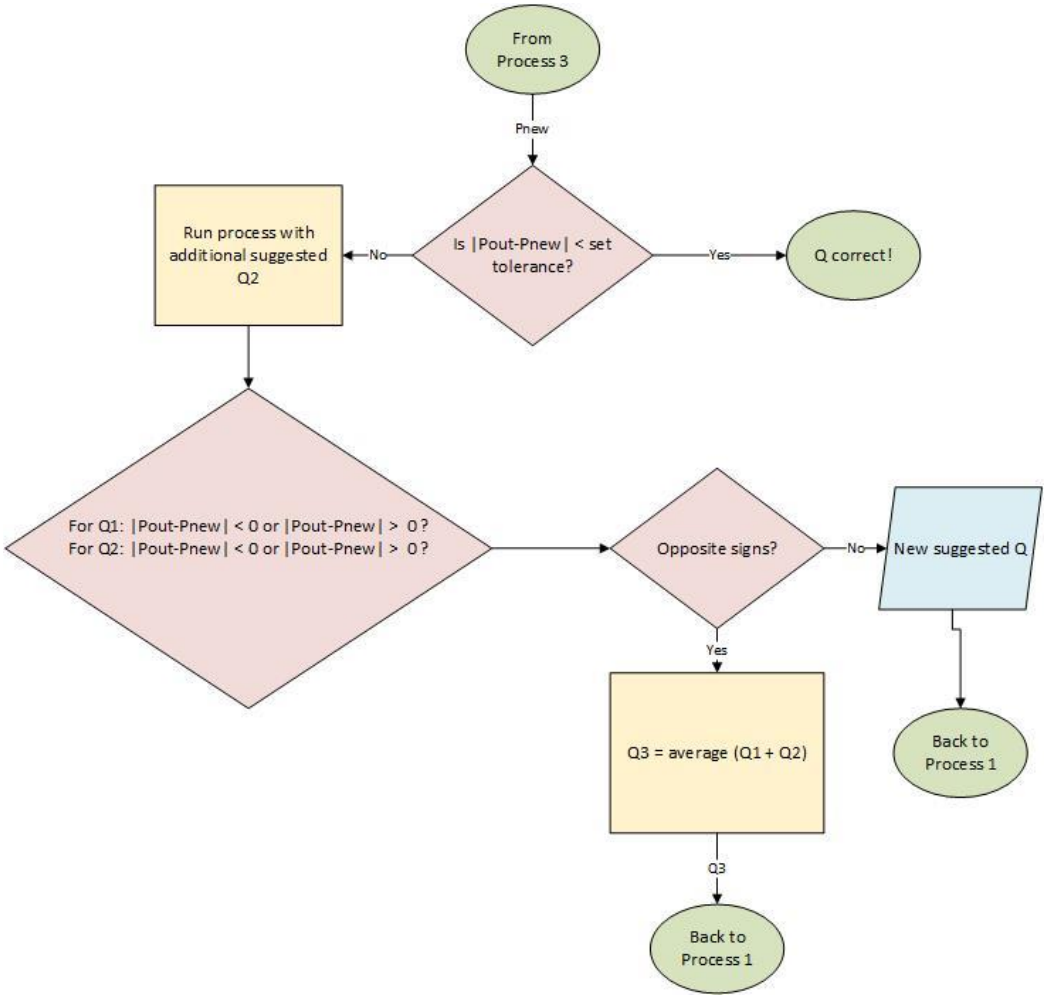

Figure 19 Process 4: Bisection Method

5.1.5 **Process Flowchart**

All four processes combined, illustrated in Figure 20, make up the whole code, which can be run for several different gas lift compositions and flow rates.

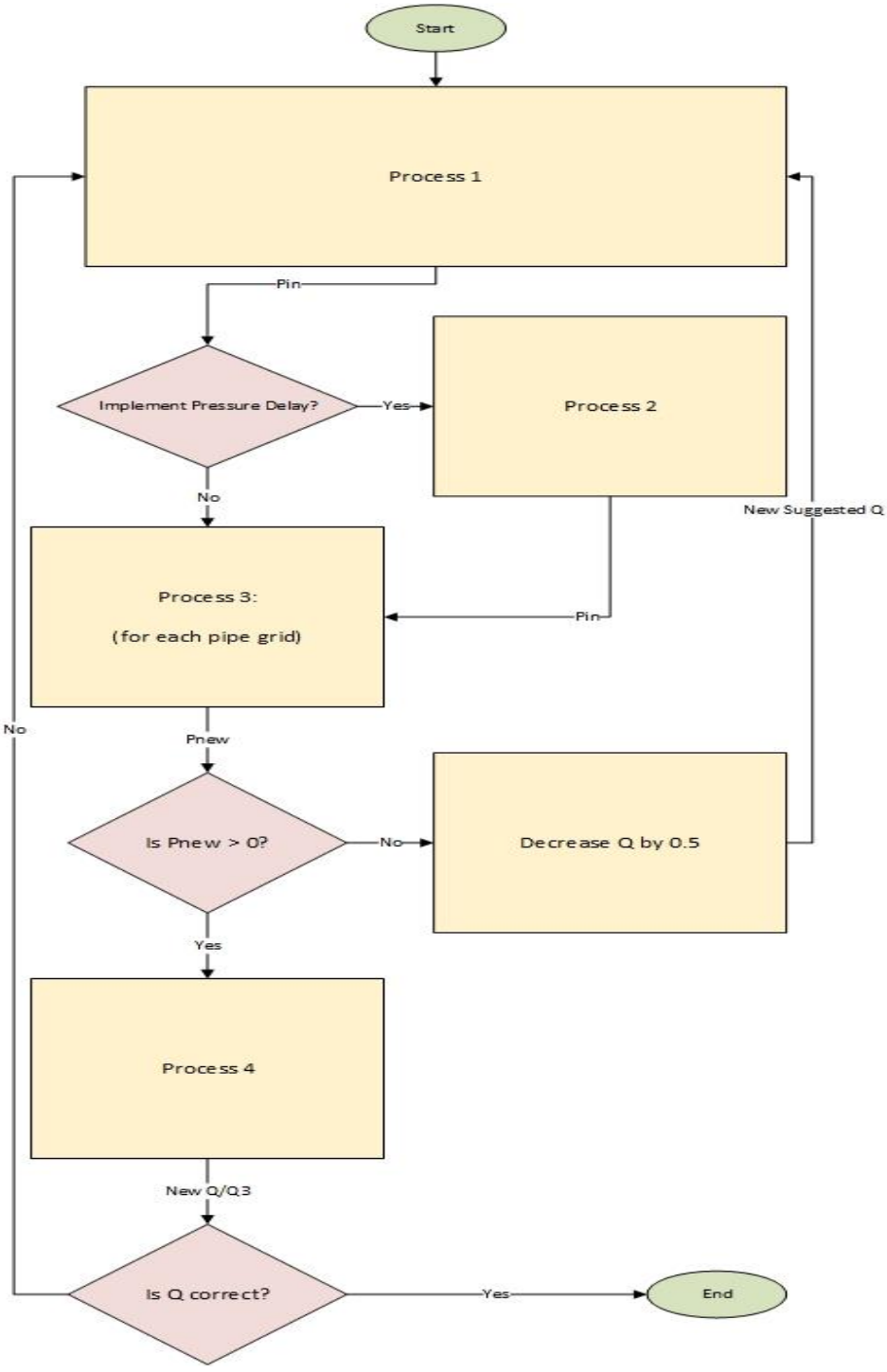

Figure 20 Complete Process Flowchart

6 SIMULATION SETUP

To explore the gas lift efficiency, Field 1, a reservoir defined in Appendix A.1 and Chapter 7, will be used as basis for the simulations, and two types of explorations will be done to study the gas lift efficiency. The simulations will have a set reservoir pressure at 120 bar and a set output pressure at 15 bar, which means locking the BHFP at 105 bar. The temperature will be held constant at 319.15 K. This simplification of conditions will not occur in a real oil field, as the flow rate is calculated at the given setting to fit the pressure drop. Normally the BHFP would change depending on the pressure drop in the pipe, which would change as the gas injection rates were increased, deciding the flow rate in the pipe. This framework will show how for the given setup and conditions the gas lift will affect the state of the system. As this is a steady state simulation, it will not show the transient effects of gas lift. The effect of mass transfer is not included in the models, though a solution or dissolution effect will be implemented to simulate a version of this.

The BHFP (P_{wf} in Figure 21) for a transient system would look like the graph in Figure 21. In the graph, the static pressure will decrease for increasing gas injection rates until it reaches the injection rate where the frictional pressure drop will dominate and thus, decrease production flow rate for even higher gas injection rates.

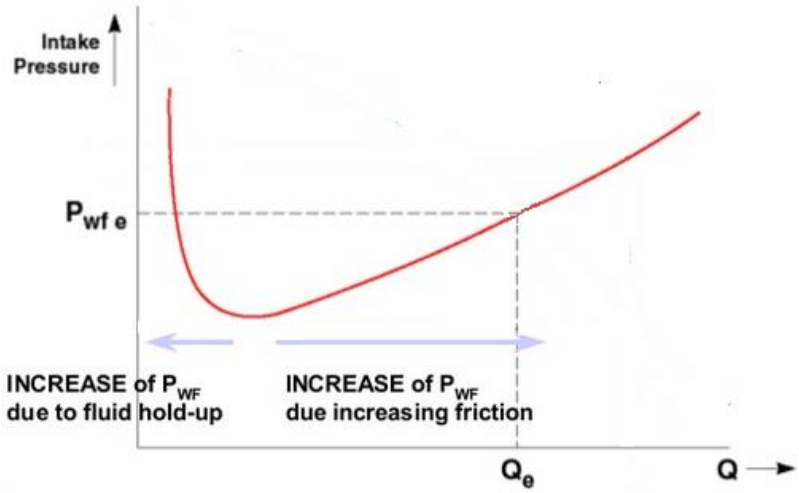

Figure 21 Well Performance Diagram (Shell, 1999)

The lowest point on the graph shows the ideal balance between the two types of pressure drop. The simulations in this thesis will be in the static dominance area, as the static pressure are still going down, see Figure 22, which shows the pressure drop for the hydrodynamic simulations.

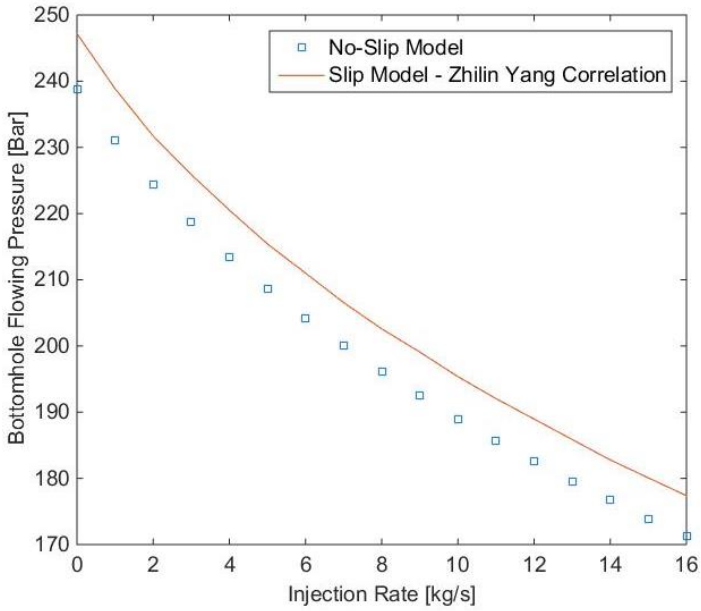

Figure 22 Pressure Drop Development for Simulations

The simulations for the vertical pipe flow requires the following input: the wellbore geometry, suggested production rate, fluid parameters supplemented by NeqSim after performing a TP-flash with the given PVT-information, and the boundary limits set by the inlet and outlet pressures, explained in further detail in Chapter 5.

6.1 HYDRODYNAMIC EXPLORATION

For hydrodynamic exploration, a simulation with the chosen void fraction correlation and slip model, plus a simulation with a non-slip model, or ideal flow, will be performed. All simulations will be run using lift-gas Mix 2, detailed in Appendix B. All values are extracted from the top grid of the wellbore.

6.2 THERMODYNAMIC EXPLORATION

For thermodynamic exploration, four simulation-variations will be tested:

1. Injection of lift-gas with varying compositions, Mix 1 and Mix 2 (presented in Appendix B).
2. Altering reservoir pressure from140 bar to 110 bar, effectively changing the BHFP from 125 bar down to 95 bar, and investigating how the change in pressure difference between the static pressure and the reservoir pressure affects the gas lift efficiency.
3. Exploring the solution effects by lowering the reservoir's bubblepoint by altering the composition, creating an undersaturated mixture. This new composition is described in Appendix A.2.
4. Pressure delay implementation; increasing pressure by a set increment when the pressure is over bubblepoint, holding the pressure equal at the bubblepoint and decreasing pressure by a set increment below the bubblepoint pressure. This is done in order to simulate an increased solution or dissolution process. Three variations will be performed:
    a. A baseline – no pressure delay
    b. Equal amount delay on both sides of the bubblepoint pressure
    c. Distinct delay on each sides of the bubblepoint pressure

The results will be plotted as lift curves, with liquid volume flow rate against an increasing mass flow rate lift-gas.

Any irregularities will be analysed through additional parameters gathered and plotted to reveal an explanation of the results.

Important term explanations for simulations:

- Undersaturation: Fluid is above bubblepoint pressure, and has the potential to absorb more gas to reach saturation pressure.
- Saturation pressure: Fluid is at bubblepoint pressure.
- Under saturated: Fluid is below bubblepoint pressure and has flashed gas, further lowering the bubblepoint pressure.

6.3 MODELS FOR SIMULATIONS

Running the previous mentioned simulations demands thermodynamical models supplied by NeqSim. The chosen model for simulations are:

- Peng-Robinson Equation of State for calculation of parameters from composition (the SRK-EoS gives a much too high bubblepoint as it divides the liquid into two separate fluids).
- Friction theory viscosity-correlation.
- Conservation of total mass
- Conservation of momentum

7 SIMULATIONS RESULTS FOR FIELD 1

All simulations were run on Field 1, where adjustments was made for the specific simulation variations. The field specifications can be found in Table 2 and Table 3. This confirms the information given in Chapter 6, as well as introducing the composition of Field 1. The oil density is initially at 1021 kg/m^3 making it a relatively heavy oil.

Table 2 Initial Conditions Field 1

P_{inlet} [bar]	120
P_{outlet} [bar]	15
T_{res} [K]	319.15
Pipe Diameter [m]	0.177
Pipe Length [m]	1492
Bubblepoint [bar]	139

Table 3 Reservoir Composition for Field 1

Component	Mole Percent	Mole Weight	Liquid Density [g/cm³]
N2	0.36		
CO2	0.4		
C1	35.07		
C2	0.17		
C3	0.06		
iC4	0.04		
C7	0.03	90.645	0.7709
C8	0.02	103.418	0.798
C9	0.18	115.361	0.8168
C10	0.46	127.087	0.8317
C11-C13	4.85	152.969	0.8575
C14-C19	19.17	200.781	0.8911
C20-C24	8.36	256.61	0.9189
C25-C29	6.42	306.011	0.9381
C30+	24.41	653.609	1.0187

7.1 HYDRODYNAMIC SIMULATIONS

Simulations for hydrodynamic exploration will be performed with 120 bar reservoir pressure, and using the no-slip model along with the Zhilin Yang slip-correlation.

In a real oil field, there will be multiphase flow in the wellbore, which affects the pipe flow and rate of production. The interfacial forces between the phases as well as the mass transfer are forces creating disturbances. For example, will transitions between flow regimes due to increased friction and lowered viscosity, and changes in the pressure drop from viscosity and density changes be a factor. Figure 23 illustrates the difference in liquid production between a non-slip and slip situation.

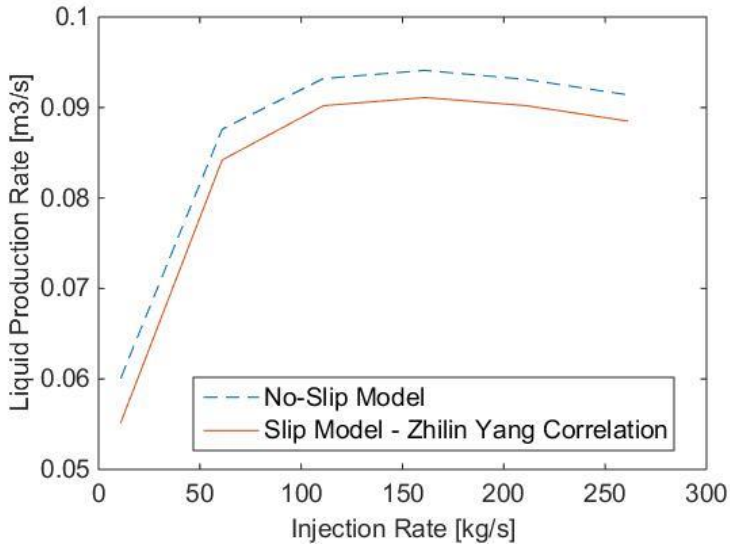

Figure 23 Liquid Production for Hydrodynamic Simulations

The production increase is 56.5 % increase for the no-slip model when using gas lift, while there is a 65 % increase for the slip model. When using the no-slip model an overestimation of 3.3 % is made for the liquid production rate, compared to the slip model. Both models give an overall similar production development for increasing gas injection rates.

Figure 24 shows that the viscosity is very much the same for both models, with a very small decline for the slip model. The GOR in Figure 25 show a slight increase in GOR for the slip model, meaning a larger expansion rate and giving more free gas for the slip model, as the void fraction will be adjusted with the Zhilin Yang Correlation and corrected for interfacial forces.

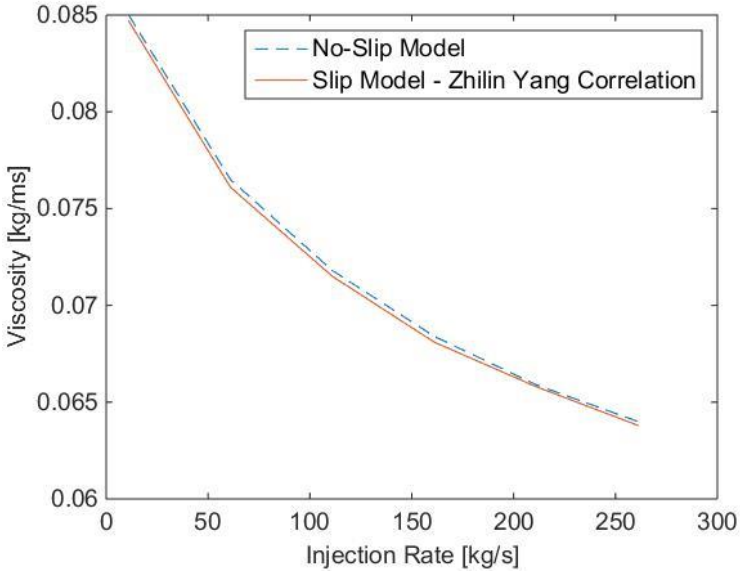

Figure 24 Viscosity for Hydrodynamic Simulations

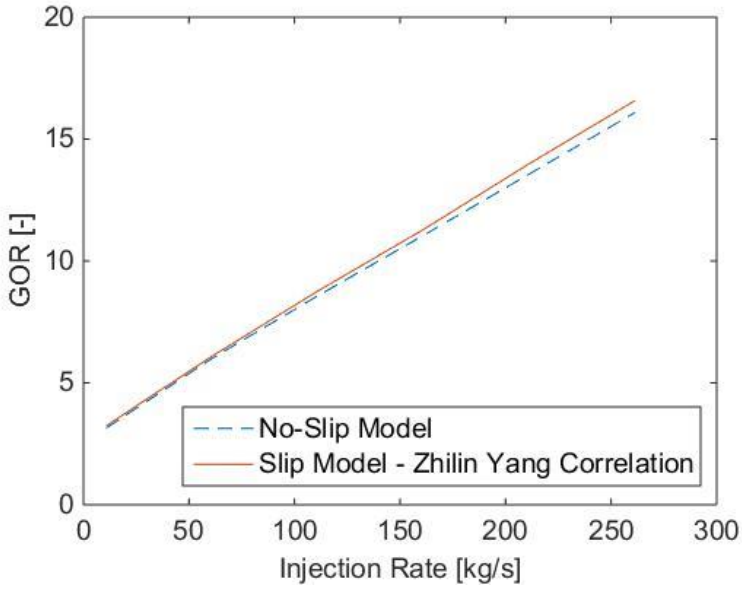

Figure 25 GOR for Hydrodynamic Simulations

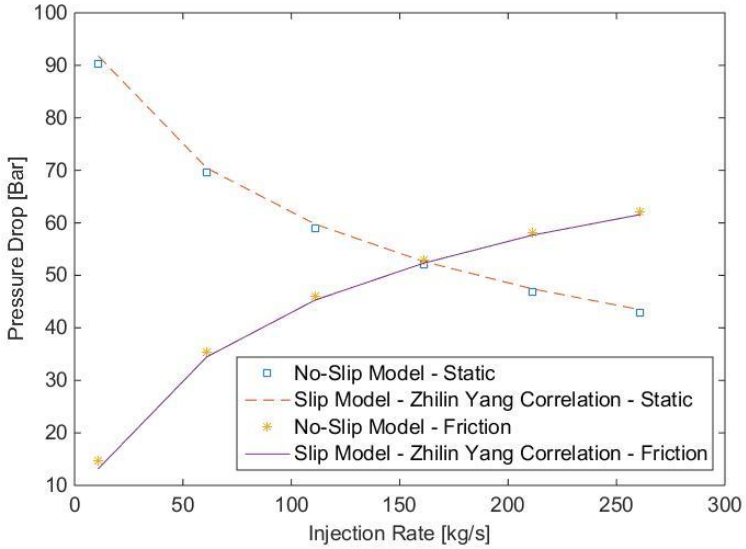

Figure 26 Static and Frictional Pressure Drop for Hydrodynamic Simulations

Figure 26 shows how the frictional and static pressure drop develops with increasing gas injection rate. As the boundary limits is set by the inlet and outlet pressure the total pressure drop will always be 105 bar, and Figure 26 shows how the two different pressure drop types divides up the total pressure drop at each gas injection rate. The static pressure drop decreases as the injection rate is amplified, lowering the density of the static column and increasing the driving force. The frictional pressure drop increases as the velocity of the fluid increases, due to increased buoyancy and lowered viscosity. As Figure 23 shows, the optimal injection rate for gas is at 150 kg/s approximately, meaning the static pressure loss is dominating in the lower region from 0 to 150 kg/s gas injection rate. Over this, the frictional pressure drop increases to a point where it will decrease the production flow rate. The model in question will use the flow rate to maintain a pressure drop up the wellbore at 105 bar. The intersection between the two types of pressure drops show the ideal balance between the two and this coincides with the optimal gas injection rate of 150 kg/s, which also seems to validate the model used for simulations.

The addition of slip in the model increases the static pressure drop, but decreases the frictional pressure drop compared to the no-slip model.

7.1.1 Discussion of Hydrodynamic Results

For analysing the results, due to the to the margin of error from computational models and assumptions made, the trends of the curves rather than the numerical values will considered,. This is to comment upon the behaviour from increased gas injection and pressure changes in the pipe.

Concluding from the hydrodynamic results, no ideal situation will occur in a real life well production and the addition of slip will decrease the production. The viscosity will be approximately the same, though the GOR will increase slightly for the slip model, meaning a higher percentage of free gas. The static pressure drop will be higher for the slip-model, while the frictional pressure drop is lower. Meaning that the frictional pressure drop will dominate the total pressure drop earlier with the slip model. There is a 65% increase in gas lift efficiency for the slip-model, which is 8.5 % more than for a no-slip model. Without accounting for slip, the production rate prediction will be 3.3% higher than what is realistic for the set conditions, which means that slip needs to be accounted for to get realistic projected values for the calculated deliverability.

7.2 THERMODYNAMIC SIMULATIONS FOR FIELD 1

This section will contain four different thermodynamic simulation variations, exploring the impact they will have on the gas lift efficiency. Section 7.2.1 will look at the effect of altering the lift-gas composition, while Section 7.2.2 studies the effect of gas lift when altering the bubblepoint of the reservoir. In Section 7.2.3, the reservoir pressure is lowered to explore the change in gas lift efficiency, before different pressure delays are applied to the simulations in Section 7.2.4. Closing out the chapter in Section 7.2.5, is the discussion of the thermodynamic simulation results.

For simulations on Field 1, there could be experimented with several variations in composition for the lift-gas. However, for the scope of this thesis, the following two compositions for the lift-gas were used, shown in Figure 27 and specified in more detail in Appendix B. Mix 1 is the heavier and denser mixture, while Mix 2 with a higher mole percentage methane, and is lighter.

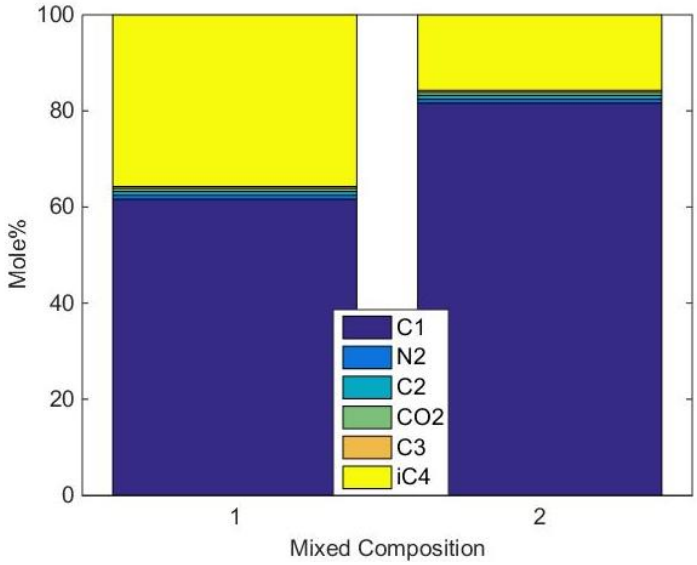

Figure 27 Lift-gas Compositions

7.2.1 Lift-gas Composition Variations

To analyse the gas lift response, a common lift curve, Figure 28, was plotted showing a clear difference in lifting efficiency when using the two different lift-gas compositions under the same conditions. The curves show a clear difference in lifting performance when using a distinct lift-gas composition.

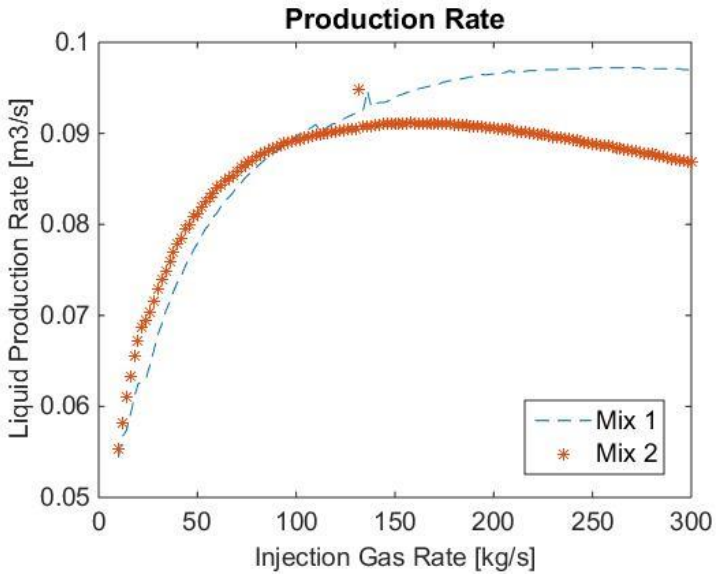

Figure 28 Liquid Production for Composition Simulation

The general lift efficiency for Mix 1 is 74.5 %, while for Mix 2 it is 65 % showing a superior response for the denser mix to the lighter one. However, the denser mix can handle a much higher injection rate of gas without decreasing production.

Mix 1 does also give a larger decrease in density and viscosity for the production fluid as Figure 29 and Figure 30 respectively shows. A higher density lift-gas composition gives a lower overall density, and produces more than for the lower density lift-gas which gives a higher density overall. This coincides with the theory of gas lift.

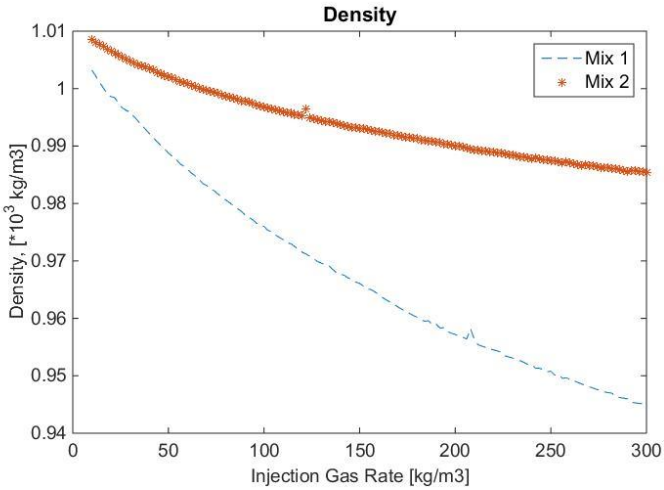

Figure 29 Density for Composition Simulations

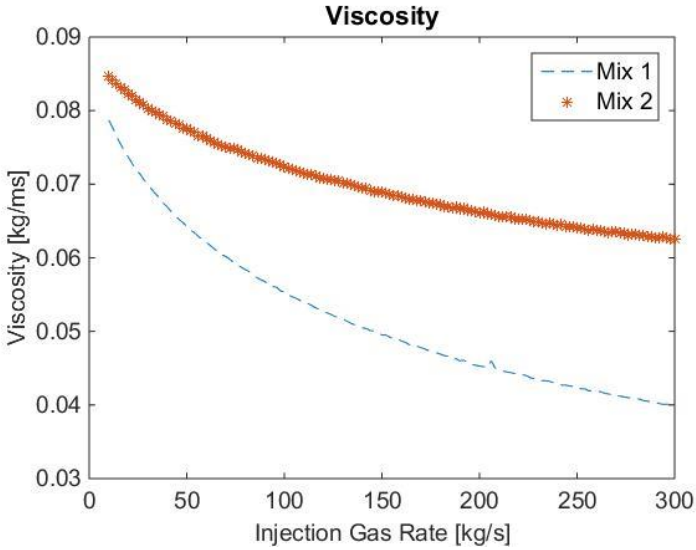

Figure 30 Viscosity for Composition Simulations

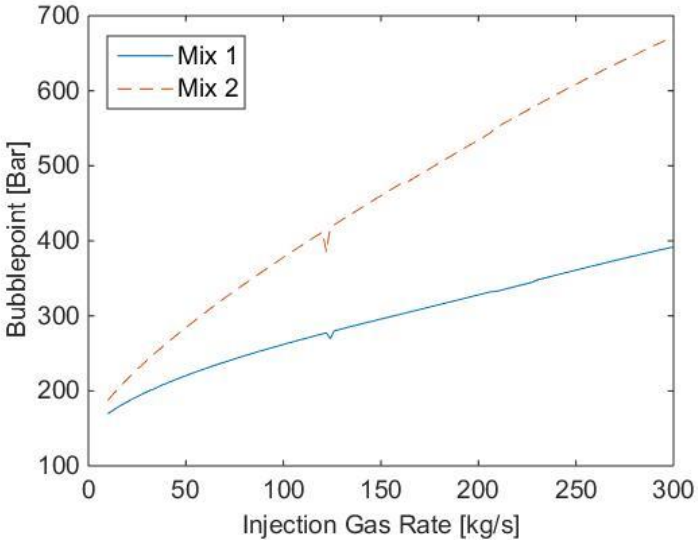

Figure 31 Bubblepoint for Composition Simulations

The bubblepoint of the two simulations is illustrated in Figure 31. Mix 2 with its lighter composition will ultimately give a much higher bubblepoint for increasing gas injection rates than Mix 1 will. Simultaneously Mix 2 will give an earlier gas expansion, which results in a larger pull on the liquid, which increases the liquid's viscosity earlier. The reservoir pressure is initially 120 bar, meaning it is below the bubblepoint pressure initially, starting out as a two-phase flow.

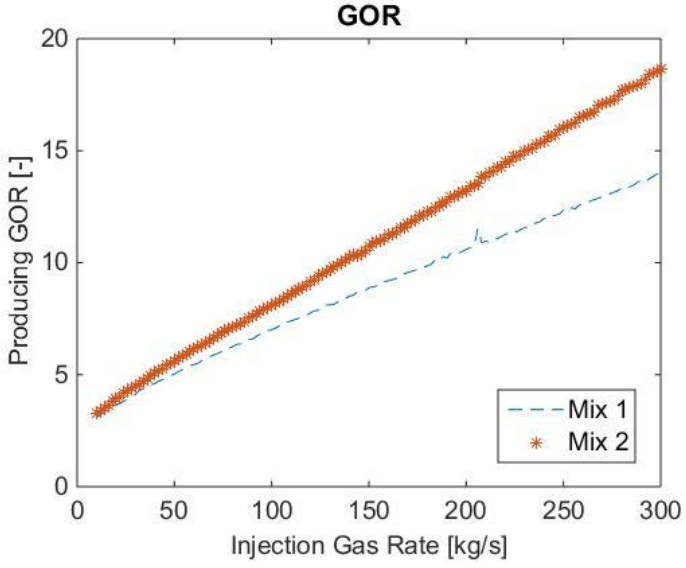

Figure 32 GOR for Composition Simulations

The GOR in Figure 32 shows little change from the modification in lift-gas composition, though it does display a higher GOR for the lighter Mix 2, giving the impression of a higher dissolution rate with the lighter mix.

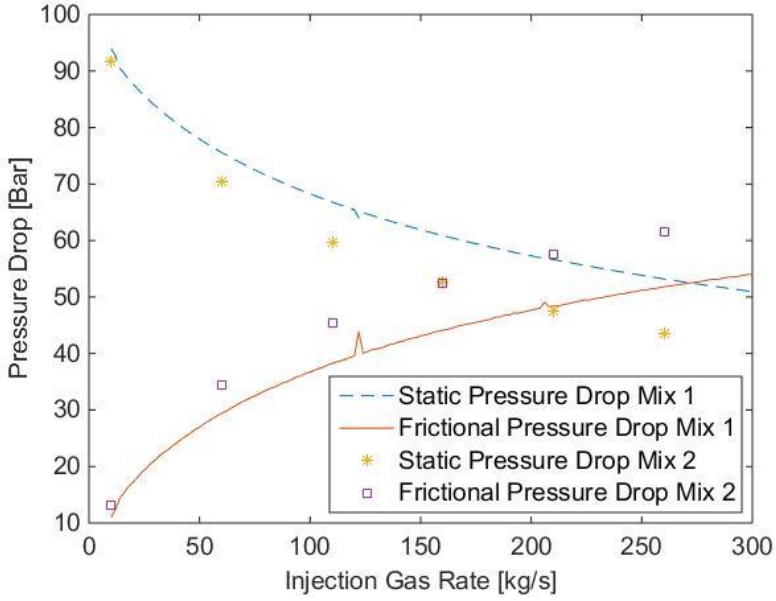

Figure 33 Static and Frictional Pressure Drop for Composition Simulations

The impact the increase of lift-gas injection has on the pressure drop is illustrated in Figure 33. It shows how the wellbores total pressure drop of 105 bar is divided between the static and frictional pressure drop with increased lift-gas injection rate. Looking at Mix 1 and Mix 2, the intersecting lines coincides with the maximum production flow rates for each lift-gas.

The intersection can be explained by looking at Figure 34. The turning point is between the hydraulic and the friction force, where the friction force will dominate the pressure drop for Mix 1 and Mix 2 after 250 kg/s and 255 kg/s, respectively.

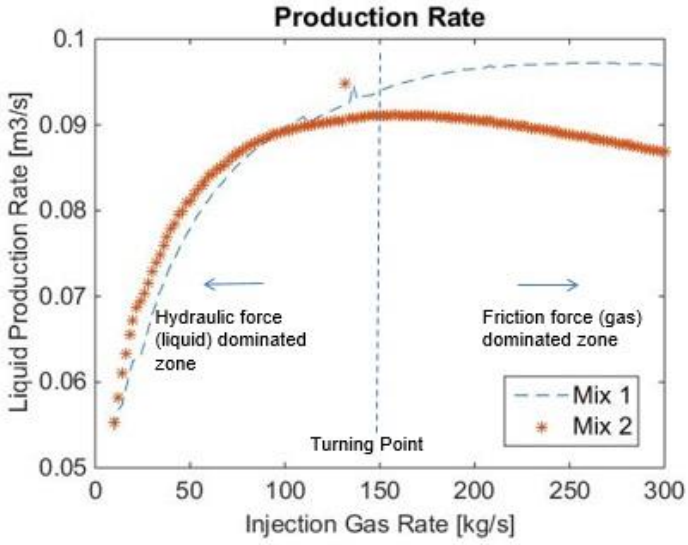

Figure 34 Dominating Zones for Pressure Drop

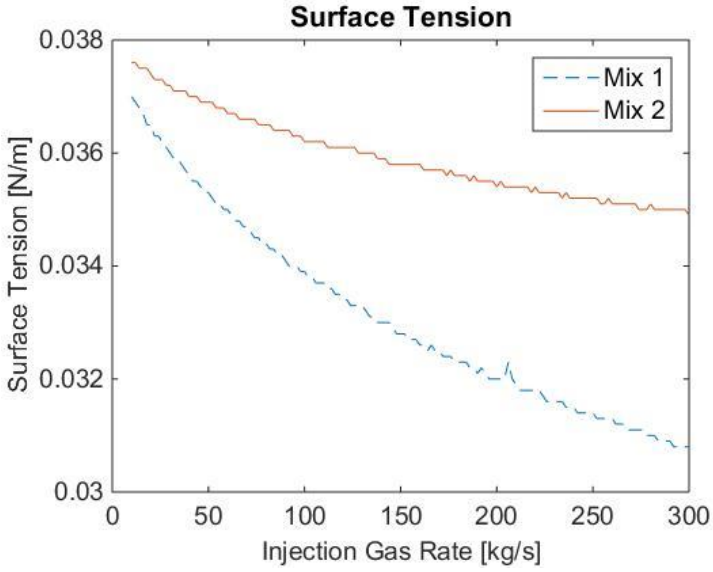

Figure 35 Surface Tension for Composition Simulations

Figure 35 shows how the surface tension is influenced in the two different simulation cases. The heavier gas has a higher solubility than the lighter gas, due to the lower interfacial tension between the two phases. The surface tension for both mixtures declines as the gas injection rate increases, suggesting a relation to the viscosity and density, as the development for the three graphs are strikingly similar. There are of course possibly more impacting conditions to the

density and viscosity behaviour, like temperature and pressure. Nevertheless, liquids with low surface tension are difficult to keep in aerosol form, giving it a lower rate of expansion.

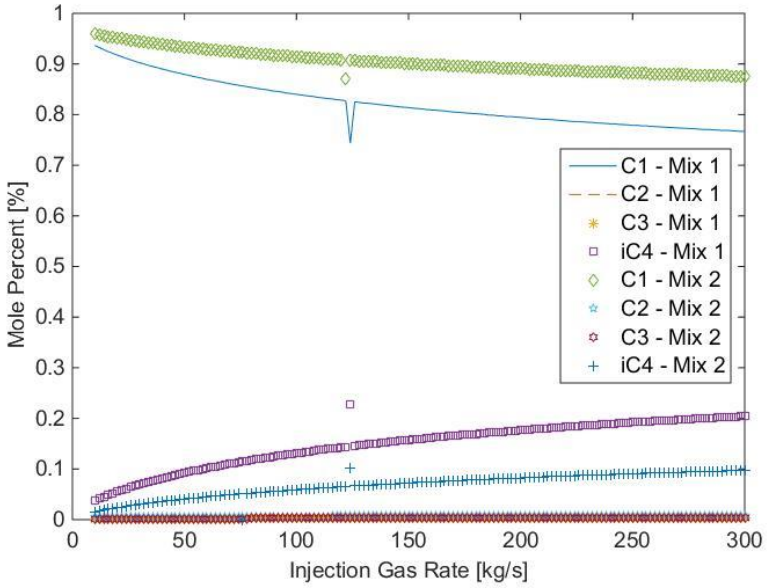

Figure 36 Mole Percent for methane, ethane, propane and isobutane in Gas Phase

The four main components in the two lift-gas mixtures are methane, ethane, propane and isobutane, as nitrogen and CO_2 are inert gases. Looking at Figure 36, showing these four components in the gas phase, it shows a clear increase of isobutane for both simulation cases, meaning with increasing gas injection rate the mole percent of isobutane in gas phase increases. It does only show a slight increase, indicating a low rate of expansion for the heavier component, though higher than for ethane and propane, which is next to negligible in the gas phase for all injection rates. As for methane, there is initially only methane released from the oil for low gas injection rates for both mixtures.

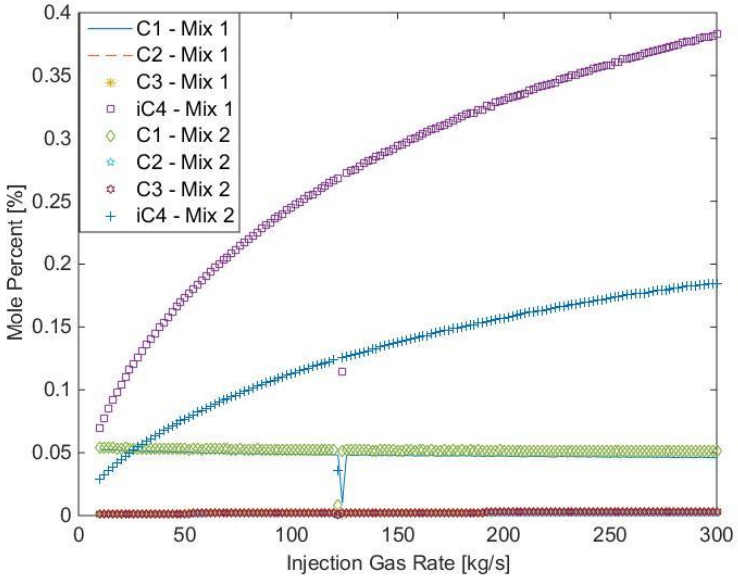

Figure 37 Mole Percent for methane, ethane, propane and isobutane in Oil Phase

In Figure 37, the same four main components are shown in the oil phase. The amount isobutane will increase with increasing rates, more so for Mix 1 as it has the higher mole percent isobutane. The figure shows a high amount of dissolution for the isobutane under the given conditions. The quantity of methane is however holding more or less stable at 0.06 mole percent, decreasing slightly for increasing gas injection rates. As for ethane and propane, the oil and gas contain already small quantities of these components and they will not influence the gas lift efficiency to any degree. As all readings are from the top of the pipe at the separator, the oil contains very little methane as it would be one of first components to evaporate, and as a result, it is the main component in the gas phase.

As Mix 2 contains more methane, which is seemingly about the only gas that expands as the pressure goes down along the wellbore. It will have a major drop in viscosity and density and the wellbore will have a much larger portion of gas, increasing the local pressure, and thereby the volumetric rate. While Mix 1 initially has a lower mole percentage of methane, and there will be a lower gas flow rate in the top of the pipe, creating a lower compressibility in the pipe and the volumetric flow rate will by that be lower. Therefore, even though the local density at the top of the pipe is higher, due to the lower density at the start and the increased local void fraction, seen in Figure 38, the lighter gas will give a higher volumetric rate of production. This establishes the fact that the composition of the lift-gas will influence the gas lift efficiency.

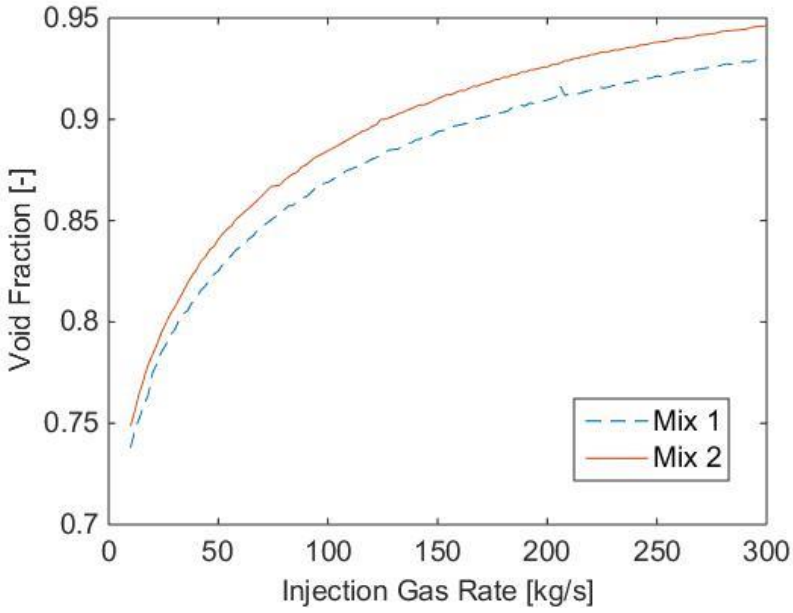

Figure 38 Void Fraction for Composition Simulations

Figure 39 shows the friction factor for simulations run with Mix 1 and Mix 2, showing initially the same trend as for turbulent flow, following the same development as for a smooth turbulent pipe flow, as shown in the Moody Chart. As for the Reynolds number, it is very high in the 10^6 range, shown in Figure 40, meaning it is outside the range of the Blasius friction factor, and can induce uncertainties in the calculations. A possibility could be to run simulations using the Fanning or Haaland friction factor. The Reynolds number is influenced by the mixed velocity, which is very high due to the high injection rate of gas.

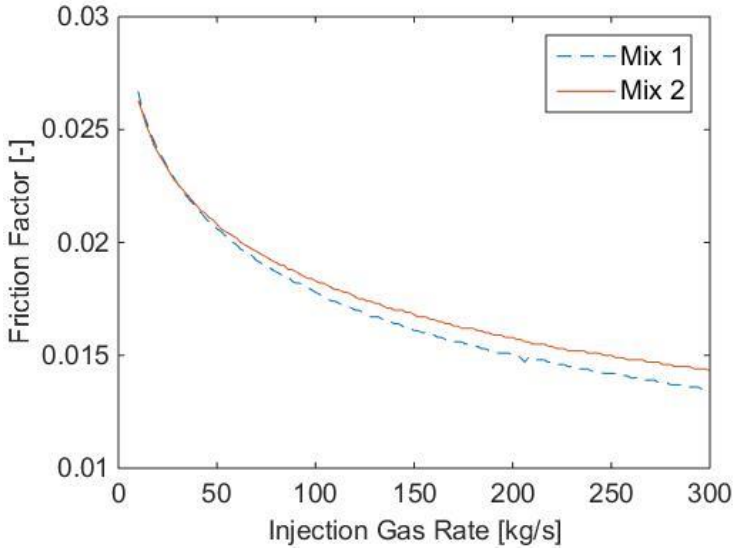

Figure 39 Friction Factor for Composition Simulations

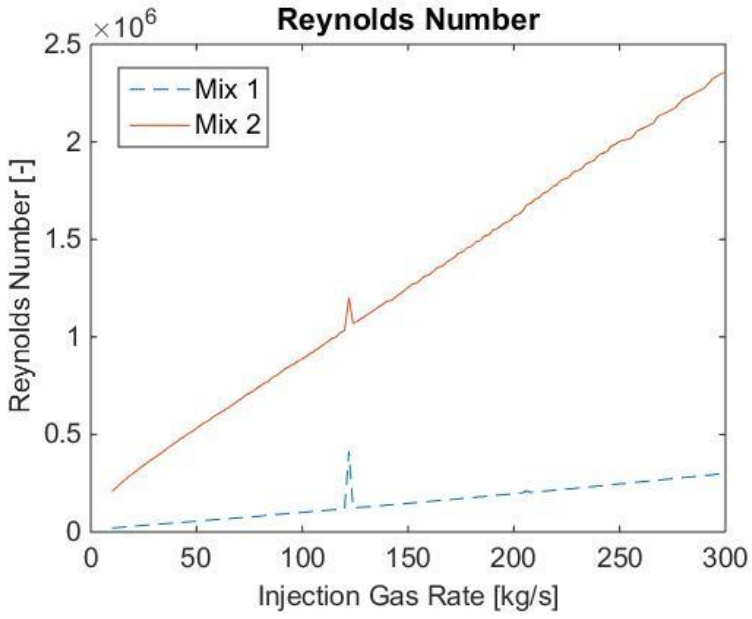

Figure 40 Reynolds number for Composition Simulations

Figure 41 and Figure 42 show the mass flow rate for the two lift-gas compositions. The gas mass flow rate is very similar for both compositions and the liquid mass flow rate shows the same trends as the volume flow rate. The figures show that in the top range of injection rate for Mix 2 the liquid mass

production rate go down, while for the same injection rate range and with Mix 1 the liquid mass production rate stabilises at around 92 kg/s.

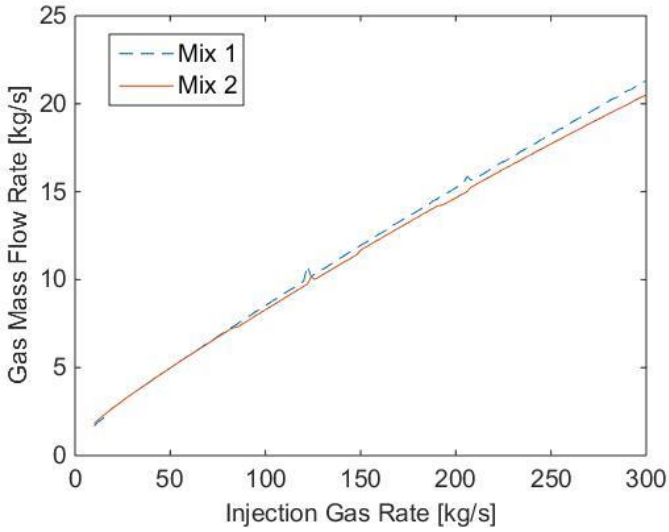

Figure 41 Gas Mass Flow for Composition Simulations

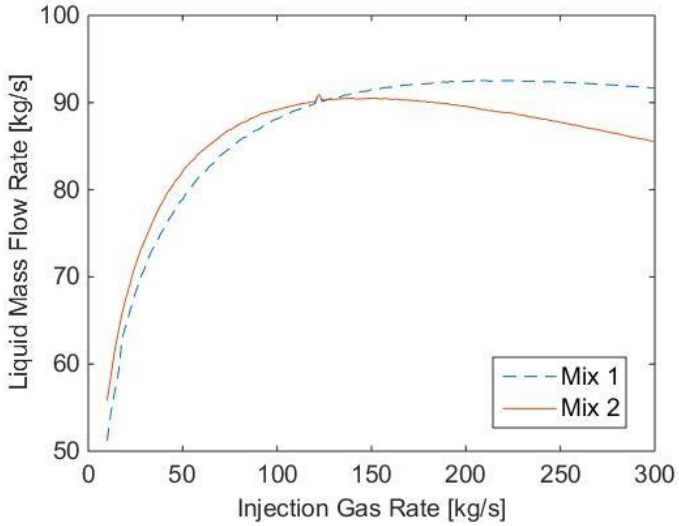

Figure 42 Liquid Mass Flow for Composition Simulations

7.2.2 Bubblepoint Alteration

Field 1 initially has a bubblepoint pressure at 139 bar found by NeqSim. This means it is a slightly under saturated reservoir, more specifically it is presumed to be around 19 bar under saturated with a reservoir pressure at 120 bar. By lowering the bubblepoint of the reservoir, the composition will be altered in order to simulate an undersaturation situation in the reservoir. The ethane and propane components have been removed, the methane mole percent lowered and several of the heavy components increased. The final composition can be found in Appendix A.2. The new bubblepoint is at 96 bar for zero injection rate, moving the reservoir from under saturated to undersaturation, giving an undersaturation level of 24 bar. The efficiency of gas lift will be explored by gas lift curves and by inspecting the GOR.

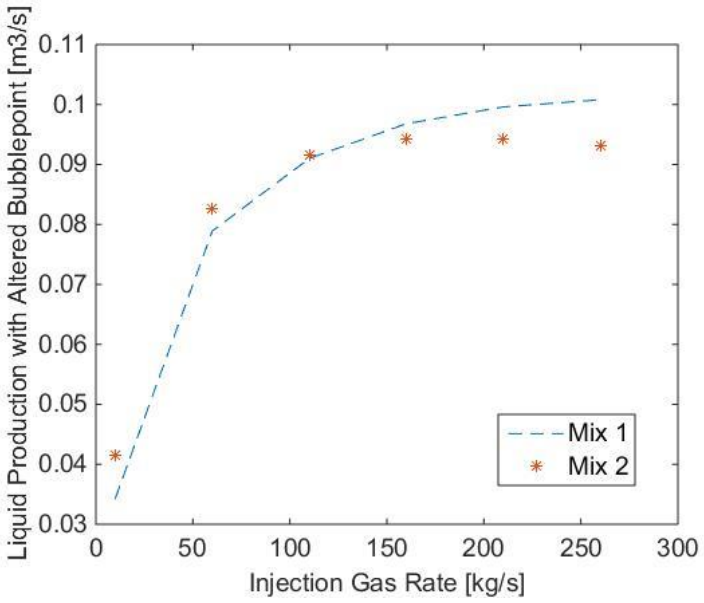

Figure 43 Liquid Production for Altered Bubblepoint Simulations

The liquid production with a lowered bubblepoint, and therefore increased undersaturation, is shown in Figure 43. The gas lift efficiency is substantially increased, with 193 % for Mix 1 and 127 % for Mix 2, explained by a higher rate of absorption above the bubblepoint pressure before expansion in the wellbore. Such an undersaturated reservoir demands a high injection rate of gas, and show a smaller decline towards the highest injection rate than for the initial reservoir. It also has a lower initial production flow rate. Mix 2 produces a constantly increasing gas lift response curve, and will need much higher injection rates before the frictional pressure gradient can overcome the static pressure gradient. The denser gas is then the more productive choice.

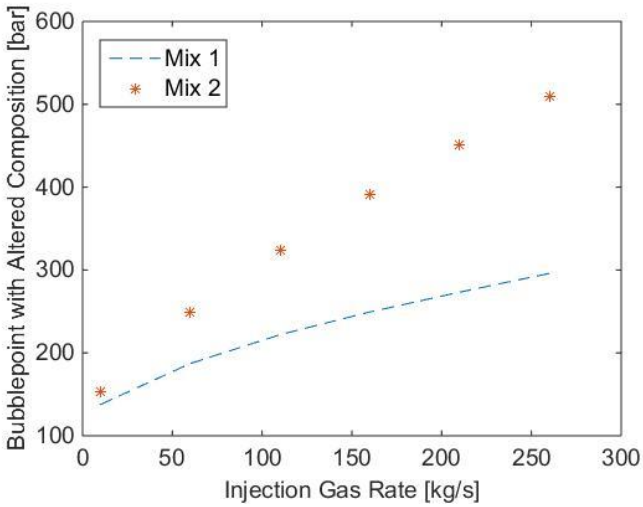

Figure 44 Bubblepoint for Altered Bubblepoint Simulations

Figure 44 shows a rapid increase in bubblepoint with Mix 2 compared to Mix 1. This is the same behaviour elicited from the unaltered composition simulation. However, as the reservoir will start out at a lower undersaturation level, the bubblepoint will initially be at a lower bubblepoint pressure, and more gas needs to be injected for the same development. The GOR, in Figure 45, shows a higher presence of gas in the wellbore as the gas injection rate increases, meaning more methane has been released.

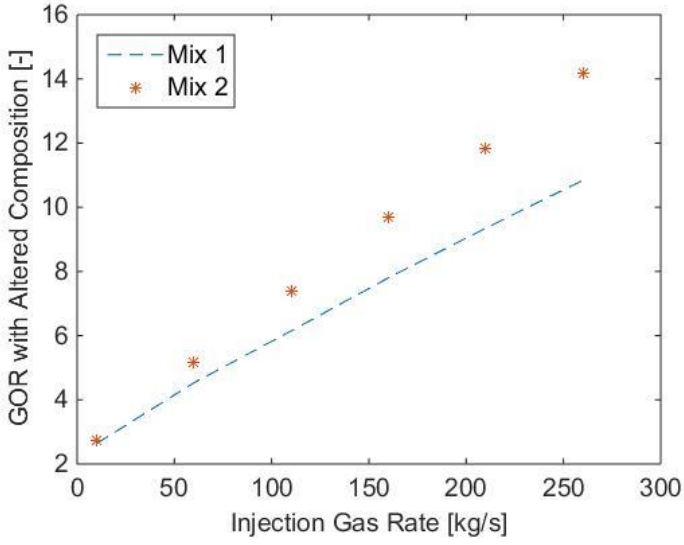

Figure 45 GOR for Altered Bubblepoint Simulations

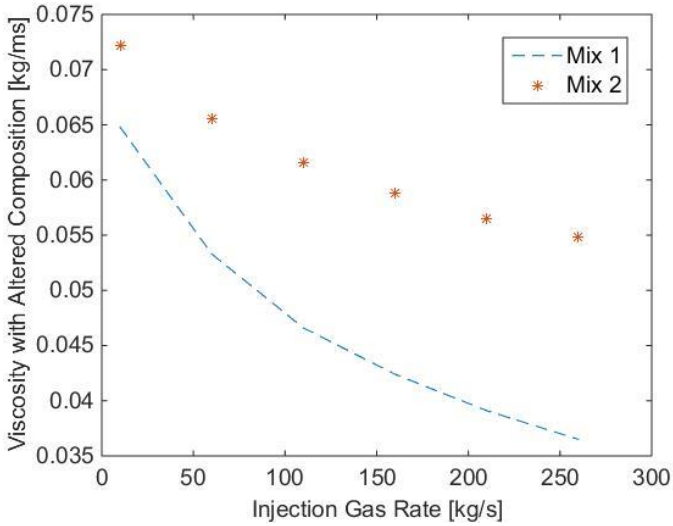

Figure 46 Viscosity for Altered Bubblepoint Simulations

The viscosity of the increased undersaturated reservoir is lower than for the initial reservoir of Field 1. Above the bubblepoint, it can potentially absorb more gas and as Figure 46 shows, at a lower bubblepoint pressure Mix 1 considerably lowers the viscosity further with increasing gas injection rates, decreasing the weight of the fluid column and increasing production.

7.2.3 Reservoir Pressure Alteration

The reservoir pressure was set to 120 bar, and will now be altered to 140 bar and 130 bar in order to see the reaction on the gas lift efficiency. The response the gas lift has to change in the reservoir pressure will be documented. As for other simulation variations run, at no or very low gas injection rates there is no production flow due to the high density of the oil and simulations will start at 10 kg/s gas injection rate. All simulations will be executed using Mix 2 for the lift-gas composition.

In Figure 47, the liquid production rate is plotted against the gas injection rate for each reservoir pressure. As the pressure of the reservoir goes down the production rate follows suit, and there is a trend of increasing injection rates for lower reservoir pressures to reach the peak production rate. The lowest production rate is initially for the lowest reservoir pressure, giving a high response for gas lift, while the highest production rate is for the highest reservoir pressure, not needing as much gas lift effect to maintain production.

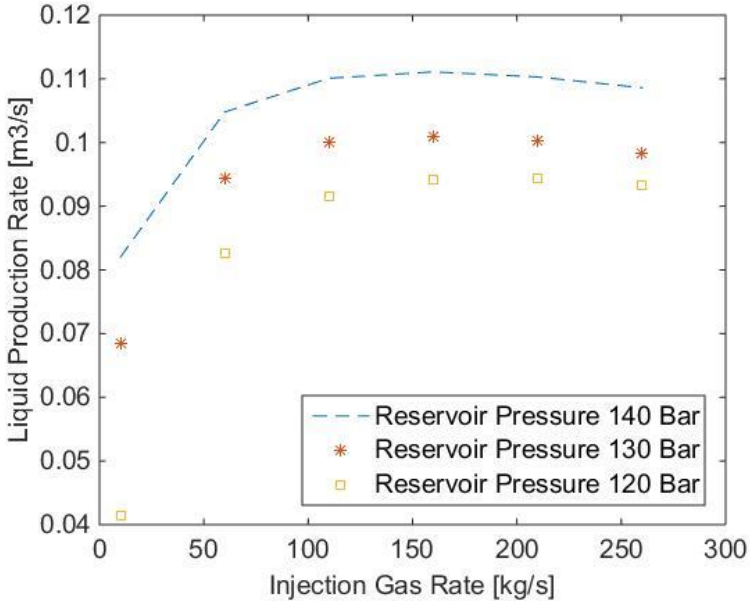

Figure 47 Liquid Production for Lowered Reservoir Pressure

Figure 48 displays how the favourable pressure difference, the driving force, increases as the gas injection rate increases. This does not include the frictional pressure drop. The higher the reservoir pressure, the higher the driving force is.

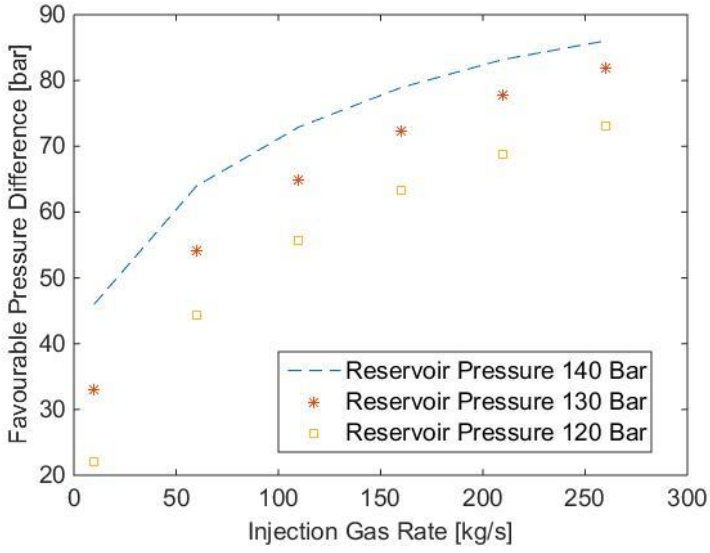

Figure 48 Driving Force for Lowered Reservoir Pressure

7.2.4 Pressure Delay Variations

The pressure delay variations will be done with lift-gas composition Mix 2 and composed of the following pressure variations in four different cases, shown in Table 4. The reservoir pressure for this simulation will be 140 bar, in order to leave room for gas expansion. Case 0 will be the baseline for comparison. With no gas injection rate, all cases will produce little to nothing at all and all simulations will start at 10 kg/s gas injection rate.

The pressure delay will be implemented in Process 2 in the programming code. Where, for every pipe grid the pressure will be set to an increment over given pressure at pressures above the bubblepoint, whilst under the bubblepoint the pressure will be reduced by an increment. At the new pressure, NeqSim will collect fluid parameters for the given conditions and these will be used for the pressure drop calculations, effectively simulating an increased dissolution or solution process.

With the rise in pressure above the bubblepoint, the viscosity and density should decrease in comparison to the baseline case, and thereby decreasing the pressure drop. Below the bubblepoint, the density and viscosity should increase compared to the baseline case, and thereby escalate the pressure drop up the pipeline.

Table 4 Case-variations for Pressure-Delay

Case No.	**Pressure delay over bubblepoint [Bar]**	**Pressure delay under bubblepoint [Bar]**
0 (Baseline)	0	0
1	2	2
2	2	5
3	10	10
4	5	10

In Figure 49, all five cases have been plotted in the same figure, comparing the production flow rate.

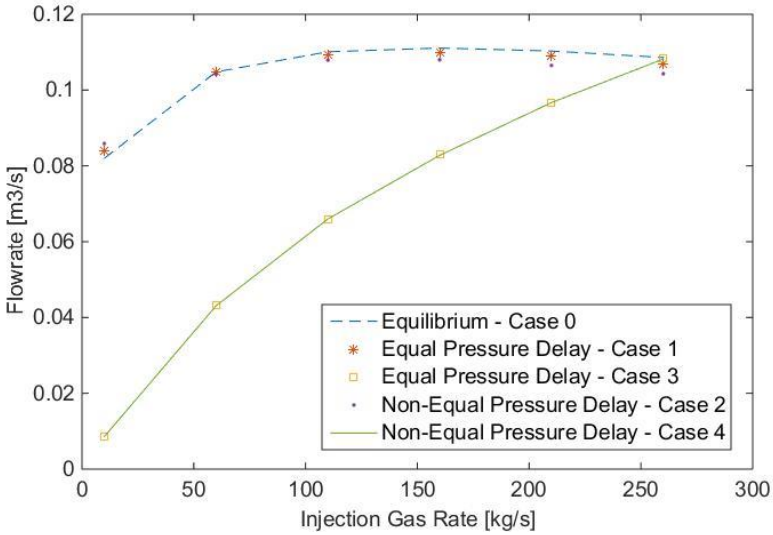

Figure 49 Liquid Production for Pressure Delay Simulations

For Case 1 and 2, with a two bar delay on both sides of the bubblepoint pressure, and two bar and five bar delay before and after the bubblepoint respectively, there is barely no change. This is mainly because the bubblepoint pressure is very close to the reservoir pressure, not giving much of a change. When increasing the dissolution effect however, up to 10 bar for Case 3 and 4, there is an equal trend for the production flow rate. It is lower for increasing flow rates than for Case 1 and Case 2, as it will expand more below the bubblepoint pressure. All four cases intersect at almost the same production flow rate for a gas injection rate of 260 kg/s. A high dissolution effect will decrease production for lower gas injection rates, but will seemingly reach the same production flow rates at higher gas injection rates.

Figure 50 shows the viscosity, as it will be affected by the solution or dissolution effects. There is next to no effect of an equal or distinct solution or dissolution effect at around two to five bars, though the distinct case will give a higher viscosity as more gas will be released below the bubblepoint pressure. When increasing the dissolution effect, however, there is a great impact on the viscosity and it will be much lower. This is because the solution is one phase and will not flash any gas. This gives a high production rate at a low viscosity. For Case 1 and Case 2 there will be more gas in the pipe, increasing the driving force for the fluid.

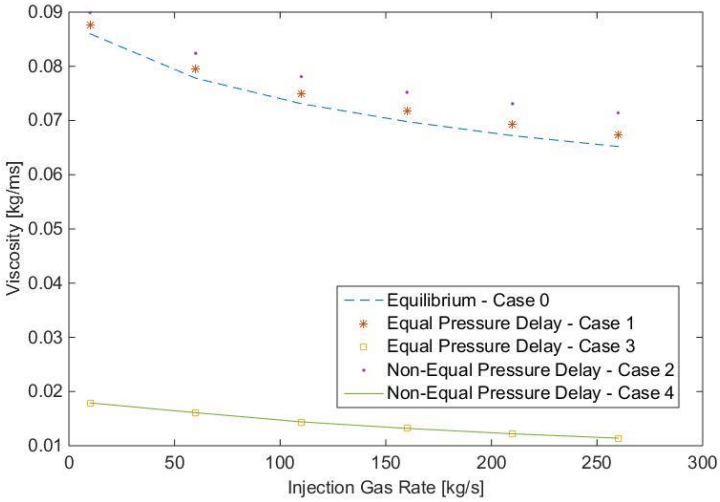

Figure 50 Viscosity for Pressure Delay Simulations

The producing GOR, shown in Figure 51, is very similar for Case 1 and Case 2, but it is zero for Case 3 and Case 4 as it will never dip below the bubblepoint. More simulations could be run for higher pressure delays, though the code's structure would need to be altered. This is because with a pressure delay input over the output pressure, there will be a negative input pressure to NeqSim that will cause the simulation to crash.

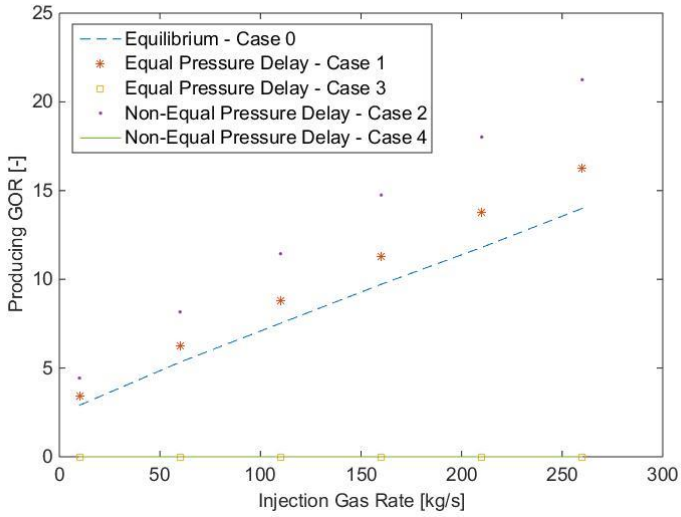

Figure 51 GOR for Pressure Delay SImulations

7.2.5 Discussion of Thermodynamic Results

The code was found to be prone to instabilities and very sluggish in relation to the addition of lift-gas. Due to the massive density of the fluid, the static pressure loss is very high and the fluid needs a high amount of injection gas to overcome this pressure drop. The code is also very sensitive of the bubblepoint, as the saturation pressure-function built into NeqSim has difficulties finding a bubblepoint when there is a high input of gas, causing the simulation to crash. This is easily adjusted by adjusting the input for suggested flow rates. Seeing as when the suggested flow rate is very low compared to the targeted flow rate, the value of the saturation pressure spikes. There are also behaviour that strays outside of what is theorised, this can possibly be explained by the high Reynolds number in the wellbore, which exceeds the range denoted for the Blasius correlation, at 10^5.

To analyse the results, the numerical values, due to the margin of error from the computational models and assumptions made, are not taken into consideration. Instead, the trends of the curves are analysed to remark upon the behaviour from increased gas injection and pressure changes in the pipe.

The four different thermodynamic simulations are discussed in the following before conclusions are drawn.

To explore the effect of different lift-gas compositions, two different lift-gas compositions were tested. It was found that a lighter lift-gas composition have a positive effect on the production flow rate as a lighter gas, such as methane, expands first and increases the gas fraction and thus the local pressure in the wellbore. Solubility increases for a denser gas, as the surface tension will be lower and as the denser gas gives a lower density and viscosity. It will also give a positive effect for gas lift, higher than for the lighter gas, though requiring a much higher gas injection rates. This can be explained by looking at the methane content of the gas as this is the main gas to expand as the pressure decreases, increasing the density and viscosity for the lighter gas simulation. Meanwhile, more of the denser gas will dissolve. As the lighter gas contains more methane this will have a large increase in both density and viscosity, giving it the higher local density and viscosity.

Undersaturation in the reservoir was simulated by changing the bubblepoint pressure of the reservoir. As the undersaturation level increases the production-rate will go down and a higher rate of lift-gas is required to reach peak performance. The production increase is at 127-193% with an undersaturated reservoir, making gas lift highly effective for such a reservoir, though requiring a higher rate of gas injection as mentioned.

When simulating an altered reservoir pressure, the BHFP changes and the production flow rate goes down. The gas lift efficiency and driving force goes up as the undersaturation level goes down. As the BHFP in a field decreases, the response of gas lift increases, though requiring higher gas injection rates and yielding lower production rates.

The pressure delay simulations yielded very different trends in the results. For a high solution and solution implementation, there is only one phase flow, giving a low viscosity and high production rates. This can be because at a five bare solution effect over the bubblepoint, the pressure only increases, never allowing for an increased dissolution effect below the bubblepoint pressure. For low solution and dissolution effects, there is a small change in production and viscosity from the equilibrium simulation since it is so close to the bubblepoint pressure.

There is a notable high value of the Reynolds number, mainly due to the high gas injection rate inducing a high mixed velocity, but this needs to be checked.

Gas lift has a positive effect on production, increasingly so with a lighter lift-gas composition and an increased efficiency on undersaturated reservoirs. At low bubblepoint pressures, the gas injection rates has to be increased to reach the same production rates.

8 SUMMARY AND RECOMMENDATIONS

8.1 MAJOR RESULTS AND CONCLUSIONS

From the two main simulation categories in this thesis, interesting discoveries were made for both the hydrodynamic and thermodynamic explorations. When studying the hydrodynamics, it appears that no ideal situation will occur in a real life well production and the addition of slip will decrease the production. There is an increase in gas lift efficiency for the slip-model, 65 %, which is 8.5 % more than for a no-slip model. Without accounting for slip, the production rate prediction will be 3.3 % higher than what is realistic for the set conditions, which makes it important to consider this in future calculations.

When looking at the thermodynamics of gas lift in vertical wells, the change in lift-gas composition was tested. It was found that a lighter lift-gas composition had a positive effect on the volumetric production flow rate as the lighter gas, such as methane, expands first and increases the gas fraction and thereby the local pressure in the wellbore. Solubility increases for a denser gas, as the surface tension will be lower. The denser gas will give a lower total viscosity and total density, which will result in a higher production flow rate, though this will require increased gas injection rates. As the lighter gas contains more methane, this will have a large increase in both viscosity and density as more gas flashes out of solution, giving it the highest local density and viscosity. It will, however have a large void fraction, increasing the local pressure and increasing the volumetric flow rate. The volumetric flow rate will differ only slightly between the two compositions, while the mass flow rate is what will govern the change in density. The composition of a lift-gas is of importance when using gas lift on a well system, and should be considered when using artificial lift.

With an increased undersaturated reservoir the production increase is at 127-193%, making gas lift highly effective for such a reservoir, though requiring a higher rate of gas injection.

When running simulations with an altered reservoir pressure, the BHFP and the gas lift efficiency changes. The gas lift efficiency and driving force goes up as the undersaturation level goes down. As the BHFP in a field decreases, the response of gas lift increases, though requiring higher gas injection rates and yielding lower production rates.

The pressure delay simulation results were inconclusive as to the gas lift efficiency due to the settings of the simulations. As the reservoir pressure was close to the bubblepoint pressure there is a very small change in the production. The effects of higher solution rates, there is a change in the pressure. This means never allowing the gas to flash, as it will not drop below the bubblepoint, keeping the flow as one phase. This effect is beneficial for production.

In conclusion, gas lift has a generally positive effect on an oil field, more so for an undersaturated reservoir, though requiring an increased gas injection rate. As for the composition of the lift-gas, it will have an impact on efficiency and should be taken into account. The delays occurring in a mass transfer situation between the phases will also affect the production, especially for a higher solution effect, and this should be studied further. From the assumptions made and the model used, it is not feasible to model all effects in a real well. The plots show indications that the production flow rate can be increased by approximately 127 % by adding approximately 150 kg/s lift-gas of a low density, and for even higher gas injection rates than simulated, there can be a much higher production for the denser gas.

8.2 LIMITATIONS

When considering the modelling work done in this thesis, where the qualitative trends have been identified and explicated, the accuracy of the predictions of the behaviour of the system will not be as good as it should be due to the assumptions made such as the constant temperature and no mass transfer. This will thus still b an approximation of the behavioural trends of changing lift-gas compositions.

The model itself is limited by the numerical frame it follows in the code. An example being that the pressure delay function is not able to simulate higher pressure-delays than around the output pressure, this resulting in negative pressure inputs to NeqSim. Due to the heavy nature of the oil, it will limit itself to no flow for the lowest input values of lift-gas, and no simulations will include this lower value.

The accuracy of the model can be increased by increasing the number of grids and lowering the tolerance, though this will give a much higher simulation time. In addition, the magnitude of the output values may be due to the simplified nature of the model, which does not account for mass transfer, pipe roughness etc., and can therefore be explained by numerical effects.

All the results will be relying on models adapted to simulate a physical situation depending on several factors that is near impossible to predict accurately, making the results an approximation. Specifically oil compositions with

components in the heaviest range can destabilise the code, depending on which viscosity correlations utilised. The viscosity variable calculated by NeqSim is a vital part of the frictional pressure drop calculations, while the density variable is commanding of the static pressure drop. Both governing the mathematical model, giving these two parameters a highly influential role and any small deviation will give big ripple effects on the results.

Due to the nature of multiphase flow and its complexity, numerical errors occurring during simulations and irregularities compared to experimental results will occur.

8.3 RECOMMENDATIONS

To further investigate the gas lift efficiency and improve results, there are several measures that can be taken, amongst them are to:

- Develop a method to analyse the simulated results in terms of non-dimensional physical parameters, from which the gas-lift efficiency is estimated is a task than is should be prioritised.
- Expand the model to include a more complex geometry, as a realistic scenario will include several different pipe angles and diameters.
- Further, advance the code to include a transport model, with heat and mass transfer and temperature variations, thus make the model more realistic, accounting for more of the natural variations occurring during pipe flow at a well site.
- Study the different composition components' effect on the lift efficiency, trying to determine the ultimate lift-gas composition for a given reservoir. Especially the impact of the lighter components as it appears as if the density will be lower for the gas lift composition with a higher mole percentage of light components.
- Run the simulations again, using the Haaland friction factor, or the Fanning friction factor to account for the high Reynolds number.
- Separate the input flow into two streams, one for the reservoir and one for the lift-gas. Integrate and couple with NeqSim in order to explore the impact of pressure changes on interfacial behaviour, such as solution or dissolution. This will make a more realistic setup of the gas lift operation as the gas flow is not integrated into the reservoir itself but will be treated as its own entity when interacting with the reservoir fluid.
- Make the code more robust by expanding the range of viscosity size and ability to handle different outcomes NeqSim produces, such as too high viscosities, too high reservoir pressure etc. In addition, alter the pressure

input for the pressure delay sequence, so it can simulate increased pressure delays.

- Compare the results for gas lift to other artificial lift methods by implementing them in the model, like for example ESP.

REFERENCES

- Aker Solutions, (2011, May 31st). Flow assurance and Multiphase Flow. Found December 3rd 2014 at https://www.akersolutions.com/PageFiles/12184/Flow%20assurance%20presentation%20-%20Rune%20Time%20I.pdf
- Bratland, O., (2009). Friction. Found 10th of June, 2015 at http://www.drbratland.com/Friction/
- Bratland, O., (2010). *Pipe Flow 2: Multi-phase Flow Assurance.* Statoil.
- Brown, K.E., (1981). *Overview of Artificial Lift Systems.* University of Tulsa, Pub. by Journal of Petroleum Technology.
- Bubbly flow in Oil, Front page image, (2015). Retrieved from http://pixabay.com/en/olive-oil-bubbles-gold-oil-food-601487/
- Conaway, C.F., (1999). *The Petroleum Industry: A Nontechnical Guide*. 1st ed., PennWell Publishing Company, Tulsa Oklahoma, USA.
- Drive mechanisms and recovery, (2014, September 5th). In AAPG. Found November 5th 2014 at http://wiki.aapg.org/Drive_mechanisms_and_recovery
- Hagedorn, A.R., & Brown, K.E. (1964, February). *The Effect of Liquid Viscosity in Two-Phase Vertical Flow*. (Published research). Found at https://www.onepetro.org/download/journal-paper/SPE-733-PA?id=journal-paper%2FSPE-733-PA
- Hu, B., G.O. Eikrem and L.S. Imsland (2001). *A study of the casing-heading problem of gas lifted wells. Technical Report 2001-6-T*. Department of Engineering Cybernetics, Norwegian University of Science and Technology.
- Kleppe, J., (2015). Review of Basic Steps in Derivation of Flow Equations, TPG4160 Reservoir Simulation, (2015). Found at http://www.ipt.ntnu.no/~kleppe/TPG4160/note2.pdf'
- La Comunidad Petrolera (September, 2011). *Diagrama de fases generalizado de la mezcla en un yacimiento de gas Condensado* (2008, September). Found May 10th 2015 at http://industria-petrolera.lacomunidadpetrolera.com/2008/09/clasificacin-de-yacimientos-en-base-los.html

- Maijoni, A., & Hamouda, A.A. (2011). *Effect of Gas Lift-gas Composition on Production Stability / Instability by Dynamic and Steady State Simulation for Continues Gas Lift Injection Mode.* Found at https://www.onepetro.org/download/conference-paper/SPE-147766-MS?id=conference-paper%2FSPE-147766-MS
- MATLAB, (undated). Found 07.05.2015 at http://se.mathworks.com/help/matlab/
- NeqSim, (undated). *NeqSim*. Found May 10th 2015 at http://folk.ntnu.no/solbraa/neqsim/NeqSim.htm.
- PetroWiki, (undated). *Oil Viscosity.* Found at http://petrowiki.org/Oil_viscosity
- Physics 6720 – Root Finding, (2012). Found at http://www.physics.utah.edu/~detar/lessons/root_finding/root_finding.pdf
- Rivera D., (2008). La Communidad Petrolera. Pressure Development in Reservoir. Retrieved from http://industria-petrolera.lacomunidadpetrolera.com/2008/09/clasificacin-de-yacimientos-en-base-los.html
- Ros, N.C.J. (1961, October). *Simultaneous Flow of Gas and Liquid As Encountered in Well Tubing.* (Published research). Found at https://www.onepetro.org/download/journal-paper/SPE-18-PA?id=journal-paper%2FSPE-18-PA
- Sawnhey, G.S., (2011). *Fundementals of Physics.* 2nd Revised edition. IK International Publishing House Pvt. Ltd, New Delhi, India.
- Shabbir, S.A. (2014, June 28th). *Viscosity reduction of heavy oils* (Published research). Found at https://www.scribd.com/doc/231674803/Viscosity-reduction-of-heavy-oils
- Shell, (1999). *Outflow*. Found 27th of May at http://www.slideshare.net/Danigarnida/1053-tubing20-performance1
- Solbraa, E., (2015). *Ikke- likevekts fenomener i olje- og gassindustrien.* Found 26th of May at http://folk.ntnu.no/solbraa/research/rapport/gassloft.htm#312
- Takácks, G., (2005). *Gas Lift Manual.* PennWell Publishing Company, Tulsa Oklahoma, USA.

- Turner, R.G., Hubbard, M.G. & Dukler, A.E., (1969). *Analysis and Prediction of Minimum Flow Rate for the Continuous Removal of Liquids from Gas Wells*. Found at http://www.ipt.ntnu.no/~curtis/courses/PVT-Flow/2013-TPG4145/e-notes/Gas-Papers/Turner-minimum-rate-to-lift.pdf
- Yang, Z., Johansen, S.T., Danielson, T.J., Dahl, A.M., (2005). *A study of void fraction with two-phase flow in large diameter pipe by using drift-flux theory*. China.
- Çengel, Y.A., & Cimbala, J.M. (2006). *Fluid Mechanics: Fundamentals and Applications.* New York: The McGraw-Hill Companies, Inc.

APPENDICES

APPENDIX A: RESERVOIR PARAMETERS

A.1: Field 1 Reservoir

Table 5 Initial Conditions Field 1

P_{inlet} [bar]	120
P_{outlet} [bar]	15
T_{res} [K]	319.15
Pipe Diameter [m]	0.177
Pipe Length [m]	1492
Bubblepoint [bar]	139

Table 6 Reservoir Composition for Field 1

	Reservoir Composition		
Component	**Mole Percent**	**Mole Weight**	**Liquid Density [g/cm³]**
N2	0.36		
CO2	0.4		
C1	35.07		
C2	0.17		
C3	0.06		
iC4	0.04		
C7	0.03	90.645	0.7709
C8	0.02	103.418	0.798
C9	0.18	115.361	0.8168
C10	0.46	127.087	0.8317
C11-C13	4.85	152.969	0.8575
C14-C19	19.17	200.781	0.8911
C20-C24	8.36	256.61	0.9189
C25-C29	6.42	306.011	0.9381
C30+	24.41	653.609	1.0187

A.2: Altered Field 1 Reservoir

Table 7 Initial Conditions for Altered Field 1

P_{inlet} [bar]	120
P_{outlet} [bar]	15
T_{res} [K]	319.15
Pipe Diameter [m]	0.177
Pipe Length [m]	1492
Bubblepoint [bar]	96 bar

Table 8 Altered Reservoir Composition for Field 1

Reservoir Composition			
Component	**Mole Percent**	**Mole Weight**	**Liquid Density [g/cm³]**
N2	0.36		
CO2	0.4		
C1	27.07		
iC4	0.04		
C7	0.03	90.645	0.7709
C8	0.02	103.418	0.798
C9	0.18	115.361	0.8168
C10	0.46	127.087	0.8317
C11-C13	4.85	152.969	0.8575
C14-C19	19.17	200.781	0.8911
C20-C24	16.36	256.61	0.9189
C25-C29	6.65	306.011	0.9381
C30+	24.41	653.609	1.0187

APPENDIX B: LIFT-GAS PARAMETERS

Field 1 Lift-gas Composition

Table 9 Lift-gas Compositions

	Mix 1	**Mix 2**
	Mole%	*Mole%*
C1	61.621	81.621
CO2	0.817	0.817
C2	0.801	0.801
N2	0.638	0.638
C3	0.398;	0.398
iC4	35.725	15.725

Altered Field 1 Lift-gas Composition

Table 10 Altered Lift-gas Compositions

	Mix 1	**Mix 2**
	Mole%	*Mole%*
C1	61.621	81.621
CO2	0.817	0.817
N2	0.638	0.638
iC4	36.924	16.924

APPENDIX C: MATLAB-CODE

```
clear all
close all
clc
clf
InitNeqSim
addpathNeqSim
processOperations.clearAll

z = 1;
y = 0;

          Add = 1.3;

for z = 2:2
    disp(z)


    press = 1;


while press < 2

for x = 113:2:206
        t = x-1;
        %t = u*0.1;

    disp(t)

GridNo = 300;
%SystemParametersField2
P_abs1 = 5;
P_abs2 = 10;
Pinlet = 120;
Poutlet = 15;
Temp = 319.15;
Pipe_D = 0.177;
Pipe_L = 1492;
Length = 1:Pipe_L;
DeltaX = Pipe_L/GridNo;
A = pi*(Pipe_D/2)^2;
g = 9.81;
P_n = Pinlet;
P_new = 0;
TOL = 0.1;
NMAX = 10000;
```

```
N = 1;
Q1 = 100;
Q2 = 105;
Q3 = 115;
Q_right = 0;
Qlift = t;

% ---------------------------------------------------------
% Matrix-list:

Equilibrium = 1;
Zuber_Findlay = 2;
Jowitt = 3;
Bestion = 4;
Zhilin_Yang = 5;
NoOfCorrelations = 5;
ChosenCorrelation = Zhilin_Yang;
%---------------------------------------------------------


Q11 = Q1;
Q22 = Q2;
Q33 = Q3;

k = 1;
Eq = 1;
Zu = 1;
Jo = 1;
Be = 1;
Su = 1;

P_Eq = 1;
P_Zu = 1;
P_Jo = 1;
P_Be = 1;
P_Su = 1;

 % Iterating between the different Correlations
for k = 5:5
    V(1,1) = Q11;
    V(1,2) = Q22;
    V(1,3) = Q33;
    if k == 1
        disp('Equilibrium Model');
    elseif k == 2
        disp('ZuberFindlay Correlation');
    elseif k == 3
        disp('Jowitt Correlation');
```

```
    elseif k == 4
        disp('Bestion Correlation');
    elseif k == 5
        disp('Zhilin Yang');
    end

while  N < NMAX

    for i = 1:length(V)
        Q = V(1,i);

        if z == 1
        %Mole Comp - Mixed Composition1 - more iButane
            C1_lg = 61.621;
            CO2_lg = 0.817;
            C2_lg = 0.801;
            N2_lg = 0.638;
            C3_lg = 0.398;
            iC4_lg = 35.725;
        else z == 2

%Mole Comp - Mixed Composition2 - more ethane, some nButane
            C1_lg = 81.621;
            CO2_lg = 0.817;
            C2_lg = 0.801;
            N2_lg = 0.638;
            C3_lg = 0.398;
            iC4_lg = 15.725;

        end

% MolePercent Composition - Field 1

N2_org = 0.36;
CO2_org = 0.4;
C1_org = 35.07;
C2_org = 0.17;
C3_org = 0.06;
iC4_org = 0.04;
C7_org = 0.03;
C8_org = 0.02;
C9_org = 0.18;
C10_org = 0.46;
C11C13_org = 4.85;
C14C19_org = 19.17;
C20C24_org = 8.36;
C25C29_org = 6.42;
C30etc_org = 24.41;
```

```
TotalStart =
N2_org+CO2_org+C1_org+C2_org+C3_org+iC4_org+C7_org+C8_org+C
9_org+C10_org+C11C13_org+C14C19_org+C20C24_org+C25C29_org+C
30etc_org;

% GasLiftAdjustment
N2_ad = N2_org*Q + N2_lg*Qlift;
CO2_ad = CO2_org*Q + CO2_lg*Qlift;
C1_ad = C1_org*Q + C1_lg*Qlift;
C2_ad = C2_org*Q + C2_lg*Qlift;
C3_ad = C3_org*Q + C3_lg*Qlift;
iC4_ad = iC4_org*Q + iC4_lg*Qlift;
C7_ad = C7_org*Q;
C8_ad = C8_org*Q;
C9_ad = C9_org*Q;
C10_ad = C10_org*Q;
C11C13_ad = C11C13_org*Q;
C14C19_ad = C14C19_org*Q;
C20C24_ad = C20C24_org*Q;
C25C29_ad = C25C29_org*Q;
C30etc_ad = C30etc_org*Q;

Total =
N2_ad+CO2_ad+C1_ad+C2_ad+C3_ad+iC4_ad+C7_ad+C8_ad+C9_ad+C10
_ad+C11C13_ad+C14C19_ad+C20C24_ad+C25C29_ad+C30etc_ad;

%NewCompositionWithGasLift
N2 = N2_ad/Total*100;
CO2 = CO2_ad/Total*100;
C1 = C1_ad/Total*100;
C2 = C2_ad/Total*100;
C3 = C3_ad/Total*100;
iC4 = iC4_ad/Total*100;
C7 = C7_ad/Total*100;
C8 = C8_ad/Total*100;
C9 = C9_ad/Total*100;
C10 = C10_ad/Total*100;
C11C13 = C11C13_ad/Total*100;
C14C19 = C14C19_ad/Total*100;
C20C24 = C20C24_ad/Total*100;
C25C29 = C25C29_ad/Total*100;
C30etc = C30etc_ad/Total*100;

MolePercentTotalNew =
N2+CO2+C1+C2+C3+iC4+C7+C8+C9+C10+C11C13+C14C19+C20C24+C25C2
9+C30etc;
```

```
% Field 1 Composition
system1 = SystemPrEos(Temp, Pinlet);
system1.addComponent('nitrogen', N2);
system1.addComponent('CO2', CO2);
system1.addComponent('methane', C1);
system1.addComponent('ethane', C2);
system1.addComponent('propane', C3);
system1.addComponent('i-butane', iC4);
system1.addTBPfraction('C7', C7, 90.645/1000.0, 0.7709);
system1.addTBPfraction('C8', C8,  103.418/1000.0, 0.798);
system1.addTBPfraction('C9', C9, 115.361/1000.0, 0.8168);
system1.addTBPfraction('C10', C10, 127.087/1000.0, 0.8317);
system1.addTBPfraction('C11-C13', C11C13, 152.969/1000.0,
0.8575);
system1.addTBPfraction('C14-C19', C14C19, 200.781/1000.0,
0.8911);
system1.addTBPfraction('C20-C24', C20C24, 256.61/1000.0,
0.9189);
system1.addTBPfraction('C25-C29', C25C29, 306.011/1000.0,
0.9381);
system1.addTBPfraction('C30etc', C30etc, 653.609/1000.0,
1.10187);

disp(z)
disp(t)

system1.createDatabase(1);
system1.setMixingRule(2);
% system1.setMultiPhaseCheck(1);
system1.initPhysicalProperties();
TPflash(system1,0);
Bubblepoint1 = bubp(system1);

            if k == 1 % Counters for the different
Correlations
                Matrix(k, Eq) = Q;
                Eq = Eq + 1;
            elseif k == 2
                Matrix(k, Zu) = Q;
                Zu = Zu + 1;
            elseif k == 3
                Matrix(k, Jo) = Q;
                Jo = Jo + 1;
            elseif k == 4
                Matrix(k, Be) = Q;
                Be = Be + 1;
            elseif k == 5
                Matrix(k, Su) = Q;
                Su = Su + 1;
```

```
    end

P_n = Pinlet;
j = 1;

    while j <= GridNo

        if P_n > 0
        system1.setTemperature(Temp);
        if z == 1
        system1.setPressure(P_n);
        else
        if press == 1
          system1.setPressure(P_n);
        % Bubblepoint for given composition
        elseif press == 2
            if P_n >= Bubblepoint1
               system1.setPressure(P_n + P_abs1);
               BPCheck(press,i) = 1;
           elseif P_n == Bubblepoint1
               system1.setPressure(P_n);
               BPCheck(press,i) = 2;
           elseif P_n <= Bubblepoint1
               system1.setPressure(P_n - P_abs1);
               BPCheck(press,i) = 3;
            end
        elseif press == 3
           if P_n >= Bubblepoint1
               system1.setPressure(P_n + P_abs1);
               BPCheck(press,i) = 1;
           elseif P_n == Bubblepoint1
               system1.setPressure(P_n);
               BPCheck(press,i) = 2;
           elseif P_n <= Bubblepoint1

              system1.setPressure(P_n - (P_n - 1));
               BPCheck(press,i) = 3;
            end
        end
        end


        TPflash(system1,0);
        system1.initPhysicalProperties();
        system1.calcInterfaceProperties();
        numberOfPhases=system1.getNumberOfPhases();
        if numberOfPhases==2
        Zgas = system1.getPhase(0).getZ();
```

```
                Zoil = system1.getPhase(1).getZ();
                molFracGas =system1.getBeta(0);
                molFracOil = system1.getBeta(1);
                gasViscosity =
system1.getPhase(0).getPhysicalProperties().getViscosity();
                oilViscosity =
system1.getPhase(1).getPhysicalProperties().getViscosity();
                gasDensity =
system1.getPhase(0).getPhysicalProperties().getDensity();
                oilDensity =
system1.getPhase(1).getPhysicalProperties().getDensity();
                surfaceTension =
system1.getInterphaseProperties().getSurfaceTension(0,1);
                %          GOR at standard conditions
                GOR =
PVTsimulation.simulation.GOR(system1);
                GOR.runCalc();
                GORstandpoint = GOR.getGOR();

                % Composition Tracking - Field 1
                N2InGas =
system1.getPhase(0).getComponent('nitrogen').getx();
                N2InOil =
system1.getPhase(1).getComponent('nitrogen').getx();
                CO2InGas =
system1.getPhase(0).getComponent('CO2').getx();
                CO2InOil =
system1.getPhase(1).getComponent('CO2').getx();
                methaneInGas =
system1.getPhase(0).getComponent('methane').getx();
                methaneInOil =
system1.getPhase(1).getComponent('methane').getx();
                ethaneInGas =
system1.getPhase(0).getComponent('ethane').getx();
                ethaneInOil =
system1.getPhase(1).getComponent('ethane').getx();
                propaneInGas =
system1.getPhase(0).getComponent('propane').getx();
                propaneInOil =
system1.getPhase(1).getComponent('propane').getx();
                i_butaneInGas =
system1.getPhase(0).getComponent('i-butane').getx();
                i_butaneInOil =
system1.getPhase(1).getComponent('i-butane').getx();

                Zg = Zgas;
                Zl = Zoil;
                MoleFraction_g = molFracGas;
                MoleFraction_l = molFracOil;
```

```
                Visc_g = gasViscosity;
                Visc_l = oilViscosity;
                Rho_g = gasDensity;
                Rho_l = oilDensity;

                MassFraction_g = system1.getWtFraction(0);
                MassFraction_l = system1.getWtFraction(1);

                Qg = MassFraction_g*Q;
                Ql = MassFraction_l*Q;

                Usg = Qg/(A*Rho_g);
                Usl = Ql/(A*Rho_l);

                Um = Usg + Usl;

%-------------------------------------------------------------
                %No-slip
 if k == 1
                Qvg = Qg/Rho_g;
                Qvl = Ql/Rho_l;
                Qvm = Qvg + Qvl;

                VolumeFraction_g = Qvg/Qvm;
                VolumeFraction_l = Qvl/Qvm;
                Visc_m = Visc_g*VolumeFraction_g +
                Visc_l*VolumeFraction_l;
                Rho_m = Rho_g*VolumeFraction_g +
                Rho_l*VolumeFraction_l;
% %                 %Zuber-Findlay drift flux correlation
 elseif k == 2
                C0 = 1.2;
                 U0 = 1.53*(g*surfaceTension*(Rho_l -
            Rho_g)/(Rho_l^2))^0.25;
                VolumeFraction_g = Usg/(C0*Um+U0); %void
fraction
                VolumeFraction_l = 1-VolumeFraction_g;
%holdup

                Visc_m = Visc_g*VolumeFraction_g +
Visc_l*VolumeFraction_l;
                Rho_m = Rho_g*VolumeFraction_g +
Rho_l*VolumeFraction_l;
%-------------------------------------------------------------

%                 Jowitt drift flux correlation
 elseif k == 3
```

```
                C0 = 1+0.796*exp(-0.061
*sqrt(Rho_l/Rho_g));
                U0 = 0.034*(sqrt(Rho_l/Rho_g)-1);
                VolumeFraction_g = Usg/(C0*Um+U0); %void
fraction
                VolumeFraction_l = 1-VolumeFraction_g;
%holdup


                Visc_m = Visc_g*VolumeFraction_g +
Visc_l*VolumeFraction_l;
                Rho_m = Rho_g*VolumeFraction_g +
Rho_l*VolumeFraction_l;

%-------------------------------------------------------------
                %Bestion drift flux correlation
 elseif k == 4
                C0 = 1;
                U0 = 0.188*sqrt((g*Pipe_D*Rho_l-
Rho_g)/Rho_g);
                VolumeFraction_g = Usg/(C0*Um+U0); %void
fraction
                VolumeFraction_l= 1-VolumeFraction_g;
%holdup


                Visc_m = Visc_g*VolumeFraction_g +
Visc_l*VolumeFraction_l;
                Rho_m = Rho_g*VolumeFraction_g +
Rho_l*VolumeFraction_l;

%-------------------------------------------------------------
%                 Zhilin Yang correlation
 else
                C0 = 1;
                U0 = 1.53*(g*surfaceTension*(Rho_l-
Rho_g)/Rho_l^2)^0.25;
                VolumeFraction_g = Usg/(C0*Um+U0); %void
fraction
                VolumeFraction_l = 1-VolumeFraction_g;
%holdup
                Visc_m = Visc_g*VolumeFraction_g +
Visc_l*VolumeFraction_l;
                Rho_m = Rho_g*VolumeFraction_g +
Rho_l*VolumeFraction_l;

%-------------------------------------------------------------
 end
```

```
                Qvl = Ql/Rho_l;
                Qvg = Qg/Rho_g;
                GORpoint = Qvg/Qvl;
%                 Qvm = Qvg + Qvl;

                Re = Rho_m*Um*Pipe_D/Visc_m;
                f_lam = 64/Re;
                f_turb = 0.316*Re^-0.25;

                    if Re > 2100
                        f = f_turb;
                        X = DeltaX*Rho_m*g;
                        ST = X*10^(-5);
                        Y =
0.5*f*DeltaX*Rho_m*Um^2/(Pipe_D);
                        FR = Y*10^(-5);
                        P_new = P_n - ST - FR;

                    else
                        f = f_lam;
                        X = DeltaX*Rho_m*g;
                        ST = X*10^(-5);
                        Y =
0.5*f*DeltaX*Rho_m*Um^2/(Pipe_D);
                        FR = Y*10^(-5);
                        P_new = P_n - ST - FR;
                    end
                else
                Zoil = system1.getPhase(0).getZ();
                oilViscosity =
system1.getPhase(0).getPhysicalProperties().getViscosity();
                oilDensity =
system1.getPhase(0).getPhysicalProperties().getDensity();
                GOR =
PVTsimulation.simulation.GOR(system1);
                GOR.runCalc();
                GORstandpoint = GOR.getGOR();
                GORpoint = 0;
                Zl = Zoil;
                Visc_l = oilViscosity;
                Rho_l = oilDensity;
                surfaceTension = 0;
     % Composition Tracking - Field 1

                N2InOil =
system1.getPhase(0).getComponent('nitrogen').getx();
                CO2InOil =
system1.getPhase(0).getComponent('CO2').getx();
```

```
                methaneInOil =
system1.getPhase(0).getComponent('methane').getx();
                ethaneInOil =
system1.getPhase(0).getComponent('ethane').getx();
                propaneInOil =
system1.getPhase(0).getComponent('propane').getx();
                i_butaneInOil =
system1.getPhase(0).getComponent('i-butane').getx();

                MassFraction_l = 1;

                Ql = MassFraction_l*Q;
                Qvl = Ql/Rho_l;
                Qg = 0;
               VolumeFraction_g = 0;
               Visc_g = 0;
               VolumeFraction_l = 1;
                Usl = Ql/(A*Rho_l);
                Usg = 0;

                Um = Usl;

                Visc_m = Visc_l;
                Rho_m = Rho_l;

                Re = Rho_m*Um*Pipe_D/Visc_m;
                f_lam = 64/Re;
                f_turb = 0.316*Re^-0.25;

                    if Re > 2100
                        f = f_turb;
                        X = DeltaX*Rho_m*g;
                        ST = X*10^(-5);
                        Y =
0.5*f*DeltaX*Rho_m*Um^2/(Pipe_D);
                        FR = Y*10^(-5);
                        P_new = P_n - ST - FR;

                    else
                        f = f_lam;
                        X = DeltaX*Rho_m*g;
                        ST = X*10^(-5);
                        Y =
0.5*f*DeltaX*Rho_m*Um^2/(Pipe_D);
                        FR = Y*10^(-5);
                        P_new = P_n - ST - FR;

                    end
```

```
            end
           else
            disp('Pressure is negative!');
            disp(P_n)
            P_n = Pinlet;
            j = 1;
            V()
            if i == 1
                V(1,i) = Q - Add;
                Q = V(1,i);

            elseif i == 2
                V(1,i) = Q - Add;
                Q = V(1,i);

            elseif i == 3
                V(1,i) = Q - Add;
                Q = V(1,i);
            end
            end
        end
          P(1,i) = P_new;
    if k == 1
        Bisection(k, P_Eq) = P_new;
        P_Eq = P_Eq + 1;
    elseif k == 2
        Bisection(k, P_Zu) = P_new;
        P_Zu = P_Zu + 1;
    elseif k == 3
        Bisection(k, P_Jo) = P_new;
        P_Jo = P_Jo + 1;
    elseif k == 4
        Bisection(k, P_Be) = P_new;
        P_Be = P_Be + 1;
    elseif k == 5
        Bisection(k, P_Su) = P_new;
        P_Su = P_Su + 1;
    end
end
disp('Pressure is: ');
P()

D1 = (P(1,1)-Poutlet);
D2 = (P(1,2)-Poutlet);
D3 = (P(1,3)-Poutlet);

if      abs(P(1,1)-Poutlet) < TOL
        Q_right = V(1,1);
```

```
            S = ['Q is correct,', num2str(V(1,1)) ,  '
kg/s!'];
            disp(S)
            break
    elseif  abs(P(1,2)-Poutlet) < TOL
            Q_right = V(1,2);
            S = ['Q is correct,' , num2str(V(1,2)), '
kg/s!'];
            disp(S)
            break
    elseif  abs(P(1,3)-Poutlet) < TOL
            Q_right = V(1,3);
            S = ['Q is correct,', num2str(V(1,3)) , '
kg/s!'];
            disp(S)
            break
    else
                    if D1 > 0 && D2 > 0 && D3 < 0  %No. 2
                        if D1 > D2  || D1 == D2
                            Q1 = V(1,2);
                            Q2 = V(1,3);
                        else
                            Q1 = V(1,1);
                            Q2 = V(1,3);
                        end
                        Q3 = (Q1+Q2)/2;
                    elseif D1 > 0 && D2 < 0 && D3 > 0 %No.
3
                        if D1 > D3  || D1 == D3
                            Q1 = V(1,3); %skal være 3
                            Q2 = V(1,2);
                        else
                            Q1 = V(1,1); %skal være 1
                            Q2 = V(1,2);
                        end
                        Q3 = (Q1+Q2)/2;
                    elseif D1 < 0 && D2 > 0 && D3 > 0 %No.
4
                        if D2 > D3 || D2 == D3
                            Q1 = V(1,3);
                            Q2 = V(1,1);
                        else
                            Q1 = V(1,2);
                            Q2 = V(1,1);
                        end
                        Q3 = (Q1+Q2)/2;
                    elseif D1 < 0 && D2 < 0 && D3 > 0 %No.
5
                        if D2 > D1 || D2 == D1
                            Q1 = V(1,3);
```

```
                        Q2 = V(1,2);
                    else
                        Q1 = V(1,3);
                        Q2 = V(1,1);
                    end
                    Q3 = (Q1+Q2)/2;
                elseif D1 < 0 && D2 > 0 && D3 < 0 %No.
6
                    if D1 > D3 || D1 == D3
                        Q1 = V(1,2);
                        Q2 = V(1,3);
                    else
                        Q1 = V(1,2);
                        Q2 = V(1,1);
                    end
                    Q3 = (Q1+Q2)/2;
                elseif D1 > 0 && D2 < 0 && D3 < 0 %No.
7
                    if D2 > D3 || D2 == D3
                        Q1 = V(1,1);
                        Q2 = V(1,2);
                    else
                        Q1 = V(1,1);
                        Q2 = V(1,3);
                    end
                    Q3 = (Q1+Q2)/2;
                elseif D1 > 0 && D2 > 0 && D3 > 0 %No.
1 and No. 8
                    disp('All Q give positive output!')
                    % P big small
                    P()
                    V()
                    Q3 = V(1,3) + Add;
                    Q2 = V(1,2);
                    Q1 = V(1,1);

                else
                    disp('All Q give negative output!')
                    %P too small
                    P()
                    V()
                    Q3 = V(1,3) - Add;
                    Q2 = V(1,2);
                    Q1 = V(1,1);

                end

    V(1,1) = Q1;
    V(1,2) = Q2;
```

```
    V(1,3) = Q3;

    end
   N = N+1;
end

end

end
    press = press +1;
end
end
```

APPENDIX D: THE BISECTION METHOD

The bisection method will be used to find the output flow rate. The method is a very simple and robust method to find the root in any continuous function. First finding two points $x = \ a$ and $x = b$ $(a < b)$ such that $f(x)$ changes sign when travelling from a to b. Assuming that $f(x)$ is a continuous function there must at least be one root between a and b. There could be instances of an odd, even or zero number of roots, so for the method to work it requires a sign change to ensure that there is at least one root. Then the midpoint between a and b is found, creating a new point c. If $f(c)$ is opposite of $f(a)$, than c is the new b. If it is the same as $f(c)$, then c is the new a. Then keep going until the interval [a - b] is less than a chosen tolerance (Physics 6720 – Root Finding, 2012).

This study uses a set output pressure to decide the varying flow rate using this method.

Figure 52 and Figure 53 show how the MATLAB-code (Appendix C) works out the correct flow rate by looking for the correct pressure. Here all correlations are shown working out which flow rate will give the correct output pressure.

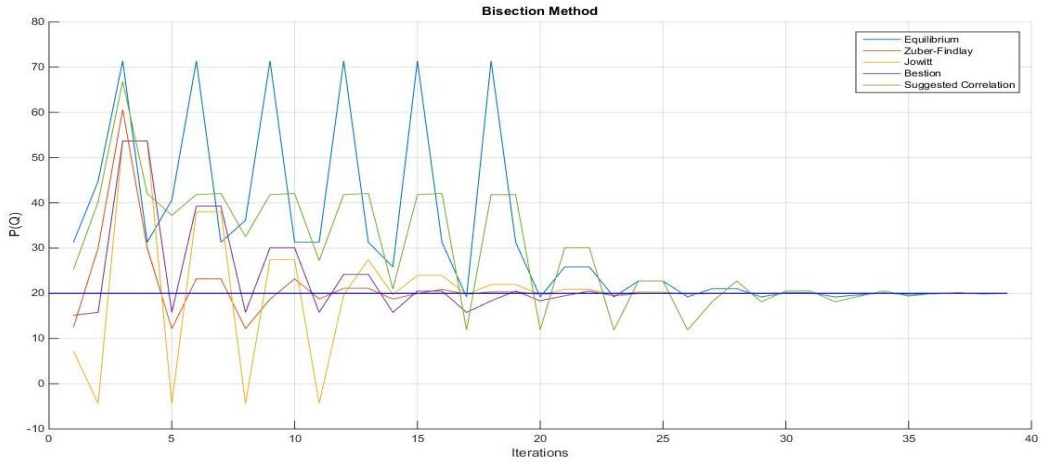

Figure 52 Pressure Development with Bisection Method

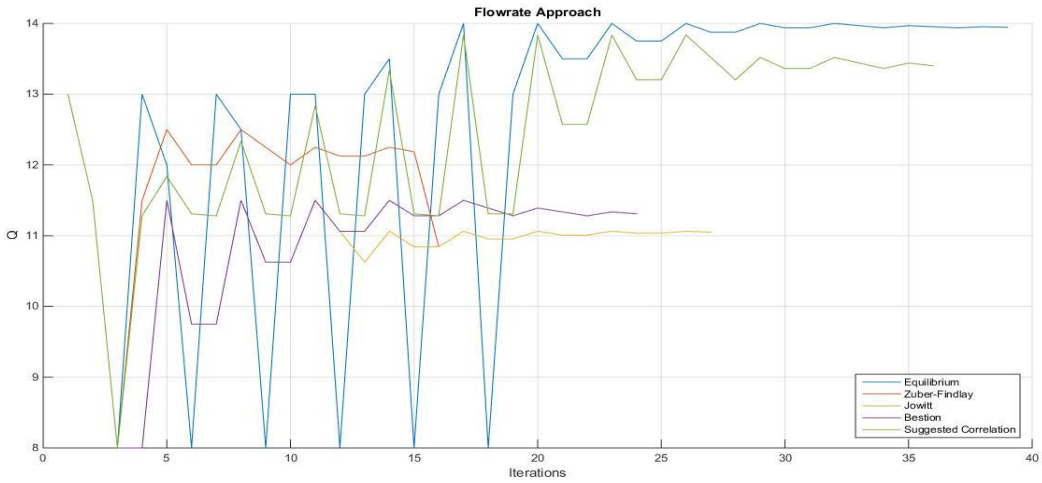

Figure 53 Flow rate Development with Bisection Method

The pressure development up the wellbore is shown for all five correlations in Figure 54, where reservoir pressure is set to a test case at 300 bar and wanted outlet pressure is set to 20 bar. Showing very little difference between the four correlations and the no-slip model, though a lower pressure in the top part of the pipe for the Zhilin Yang-correlation, substantiating the findings from Section 3.1.2.

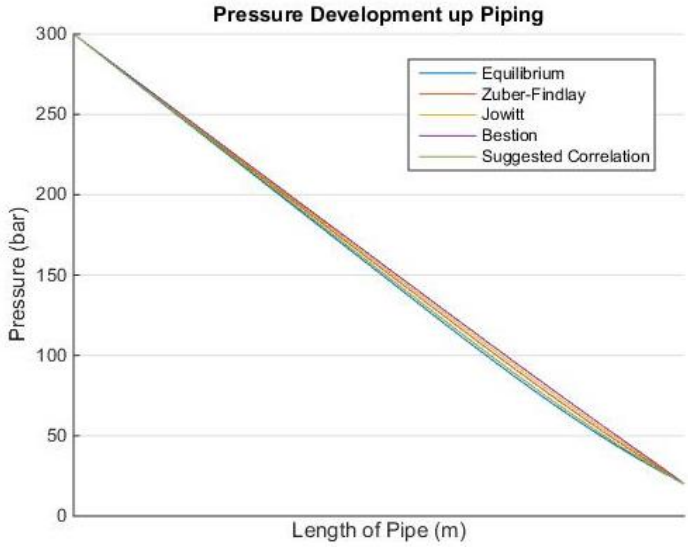

Figure 54 Pressure Decrease in Pipe for All Correlations